

Electron hopping in a soliton band: Conduction in lightly doped $(\text{CH})_x$

S. Kivelson

Department of Physics, University of California, Santa Barbara, California 93106

(Received 15 December 1980; revised manuscript received 30 November 1981)

On the basis of both theoretical and experimental studies, it has been suggested that the low-energy charge-excitations introduced into polyacetylene by light doping are charged solitons. However, these solitons are normally bound to oppositely charged impurities so that soliton conduction is inefficient at room temperature and below. In the presence of both charged and neutral solitons an alternative conduction mechanism is possible; phonon-assisted hopping between the localized electronic midgap states associated with the soliton. This is a novel process as it involves hopping between dynamical defects. The theory of this process is developed in detail in terms of a three-dimensional generalization of the microscopic model of Su, Schrieffer, and Heeger, and found to be consistent with experiment. Because of the disorder, namely the random distribution of impurities, the conduction pathways are essentially three dimensional, with interchain hops dominating intrachain hops.

I. INTRODUCTION

Since it was suggested that domain-wall, or soliton, excitations may play an important role in determining various magnetic and transport properties of undoped and lightly doped *trans*-polyacetylene, considerable theoretical¹⁻⁸ and experimental⁹⁻¹⁶ interest has focused on exploring the consequences of the soliton model. The model, however, has not been universally accepted, partially due to its seeming inability to account for the observed temperature and field dependences of the conductivity and thermopower (and partially due to some controversy concerning certain of the experimental data¹³). Thus, it is our purpose in this paper to study the transport properties of lightly doped polyacetylene within the context of the soliton model, and then to make a cursory comparison between theory and experiment. In addition, some novel aspects of the low-temperature conduction mechanism, electron hopping between dynamical defects, make the problem quite interesting in its own right, independent of any particular model system. A brief preliminary report on this work is contained in Ref. 7.

The soliton model of *trans*-polyacetylene has been explored extensively by Su, Schrieffer, and Heeger¹ (SSH) and others. They show that a single strand of polyacetylene can be treated approximately as a chain of atoms with one Wannier func-

tion of each spin per atom, corresponding to the carbon π orbital. (The σ electrons are adiabatic slaves to the ionic coordinates, and excitations of the σ system play little role in the physics.) Undoped polyacetylene, shown schematically in Fig. 1(a), has one electron per carbon. A Peierls distortion with a period of two lattice constants (dimerization) opens up a band gap of $2\Delta_0$ in the electronic spectrum at the Fermi energy, and hence makes the system an insulator [see Fig. 2(a)]. Because Δ_0 is large compared to a typical phonon energy, the electronic and ionic parts of the problem can be factored within the Born-Oppenheimer approximation. Two different senses of the dimerization are possible, one in which even numbered carbons move to the right (*A* phase), the other in which they move left (*B* phase), hence there are two degenerate ground states. A soliton is the boundary between a region of *A* phase and *B* phase, as shown schematically in Fig. 1(b). The picture is somewhat misleading as the actual soliton width, $2\xi_0$, is estimated by SSH to be about 15 lattice constants. Associated with the soliton is a localized midgap (nonbonding) electronic state, as shown in Fig. 2(b). In the neutral soliton, this midgap state is singly occupied, hence the soliton has spin $\frac{1}{2}$. If a second electron is added to the midgap state or if the original electron is removed, a charged soliton with spin 0 remains. Polyacetylene also exists in another isomer, *cis*- $(\text{CH})_x$ shown schematically in

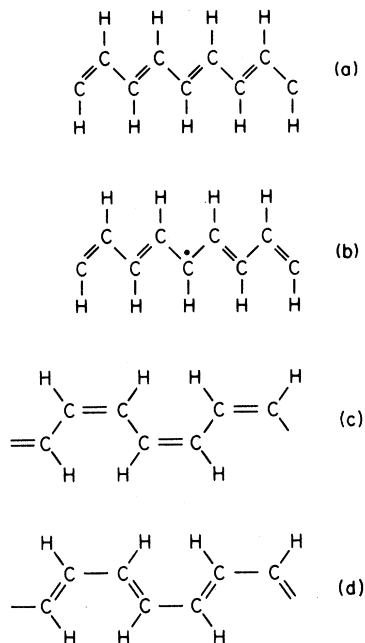


FIG. 1. Schematic representation of a piece of a neutral transpolyacetylene chain; (a) perfectly dimerized, and (b) containing a soliton and a single, unpaired, non-bonding electron. (b) is somewhat oversimplified as the actual soliton is spread out over about 15 lattice sites. (c) and (d) show schematically the two possible, inequivalent bonding configurations of *cis*-polyacetylene.

Figs. 1(c) and 1(d). *cis* differs from *trans* in that the two senses of the dimerization are inequivalent. Thus, single solitons are energetically forbidden in *cis*-(CH)_x. The present theory, therefore, pertains only to *trans*-(CH)_x.

In undoped and lightly doped polyacetylene there is a small number of neutral solitons. Their concentration¹⁰ (typically of order one per 3000 carbons in undoped polyacetylene) can be estimated quite accurately from the Curie-law susceptibility to which they give rise.¹⁷ There is evidence from ESR and NMR experiments that they are quite mobile, which suggests a small soliton effective mass (SSH estimate that $m^* \approx 6m_e$). Upon doping, charge is transferred from the dopant to the polyacetylene chain, either by changing the occupancy of a preexisting neutral soliton¹⁷ or by the induced creation of a new, charged soliton.¹⁸ A charged soliton, too, would be quite mobile, were it not for the fact that it is bound rather strongly to the remaining charged impurity by their mutual Coulomb attraction with binding energy E_b . Estimates due to SSH of the various parameters which enter the model are summarized in Table I. The

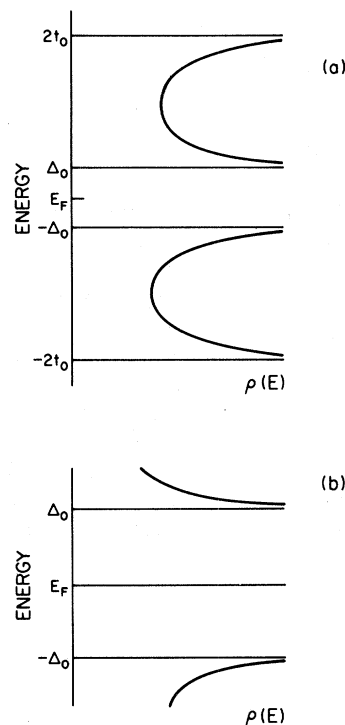


FIG. 2. Schematic representation of the density of states of a polyacetylene chain: (a) perfectly dimerized, and (b) containing a soliton. The position of the Fermi energy is appropriate to a neutral chain.

estimate of $E_b \sim 0.3$ eV was obtained by SSH assuming that the electronic charge is screened by the full in-chain dielectric constant κ which is found experimentally to be about 10. The screening at the short distances involved which is probably less than the full dielectric screening, so the 0.3 eV is probably an underestimate of E_b .

Spin diffusion at all temperatures of interest is dominated by the motion of the neutral solitons (characterized by a neutral soliton diffusion constant D_n). This motion is highly one dimensional as the soliton is a topological excitation and so cannot hop between chains. We shall see that a small amount of spin diffusion perpendicular to the chain (three-dimensional diffusion) is possible due to electrons hopping between solitons.

Charged transport is somewhat more complicated. At high temperatures, it is presumably dominated by charge-soliton diffusion. However, only those charged solitons that are not bound to a charged impurity (dopant) contribute to the conductivity. As shown in Sec. IV their contribution to the conductivity is

$$\sigma_{\text{sol}} \sim \frac{e^2}{k_B T} D_{\text{ch}} e^{-E_b/k_B T}, \quad (1)$$

TABLE I. Physical parameters of polyacetylene and other frequently used symbols.

| Physical parameters | | | |
|-------------------------|--|-----------------|-----------|
| Parameter | Description | Estimated value | Reference |
| $4t_0$ | π bandwidth | 10 eV | SSH |
| $2\Delta_0$ | band gap | 1.4 eV | SSH |
| a | chain length per carbon | 1.22 Å | SSH |
| b | interchain separation | 4.39 Å | Ref. 10 |
| $\xi_{ }$ | in-chain electron decay length | $7a$ | SSH |
| ξ_{\perp} | out-of-chain electron decay length | 2.3 Å | Appendix |
| N | typical number of carbons per chain | 3000 | Ref. 10 |
| E_b | soliton binding energy to a charged impurity | > 0.3 eV | Sec. IV |
| $\hbar\omega_0$ | typical optical-phonon frequency | 0.15 eV | MR |
| $\hbar\omega_1$ | soliton vibrational energy | 0.06 eV | SSH |
| $\hbar\Delta\omega$ | half-width of optical-phonon spectrum | 0.05 eV | MR |
| c | speed of sound | | MR |
| Other important symbols | | | |
| Symbol | Description | Defining Eq. | |
| σ_{sol} | Free-soliton contribution to the conductivity | (1) | |
| σ_{hop} | Hopping contribution to the conductivity | (2) | |
| D_n | Neutral-soliton diffusion constant | (59) | |
| D_{ch} | Charged-soliton diffusion constant | (1) | |
| y_n | Concentration of neutral solitons per carbon | | |
| y_{ch} | Concentration of charged solitons per carbon | | |
| c_{imp} | Concentration of charged impurities per unit volume | | |
| $\gamma(T)$ | Hopping-rate prefactor | (28) and (57) | |
| $\mathcal{S}(\vec{R})$ | Electronic-overlap integral between soliton bound states | (24) and (27) | |
| λ_{α} | Nonadiabatic electron-phonon coupling constant | (12) | |
| $g(E)$ | Electron-phonon coupling function | (22) and (55) | |

where the exponential factor reflects the fraction of solitons that are “free” [see Eq. (61)]. D_{ch} is the diffusion constant of a free charged soliton.

At low temperatures the number of free solitons is so small that a conduction mechanism with a smaller activation energy takes over. Consider, for instance, a negatively charged soliton bound to a positively charged impurity on one chain and a neutral soliton on another, nearby chain. It is always possible for the electron to make a phonon-assisted transition, or “hop,” from the charged soliton to the neutral soliton. If the neutral soliton is isolated (that is, far from any charged impurity), this process is energetically as costly as liberating a charged soliton from an impurity. However, if the

neutral soliton happens to be near another impurity, a situation shown schematically in Fig. 3, then the energetic cost is much reduced. The resulting conductivity, as derived in Sec. III is

$$\sigma_{\text{hop}} \approx A \frac{e^2 \gamma(T)}{k_B T N} \left[\frac{\xi}{R_0^2} \right] \frac{y_n y_{\text{ch}}}{(y_n + y_{\text{ch}})^2} e^{-2BR_0/\xi}, \quad (2)$$

where A and B are pure numbers [see Eq. (38)], $\gamma(T)$ is a frequency defined in Eq. (28), $c_{\text{imp}} = (\frac{4}{3} \pi R_0^3)^{-1}$ is the concentration of charged impurities, ξ is an average decay length of the electronic wave function defined in Eq. (37), y_n and y_{ch} are the concentration of neutral and charged solitons per carbon atom, and N is the number of

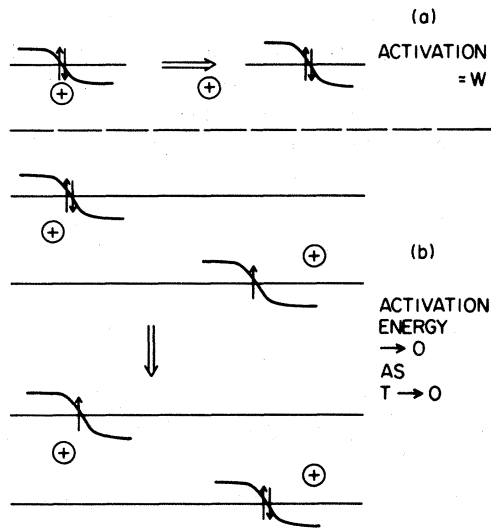


FIG. 3. Schematic representation of soliton conduction. (a) Free-soliton conduction in which a bound charged soliton is thermally liberated. (b) Hopping of an electron between soliton bound states. The \oplus represents a positively charged impurity, \ominus represents a soliton, and the arrows represent electrons of given spin orientation in the soliton bound state.

carbons per polyacetylene chain. $\gamma(T)/N$ is a characteristic frequency which is proportional to the fraction of time a pair of solitons are so situated that the initial and final soliton states are within about $k_B T$ of each other. The final exponential factor reflects the electronic overlap between two solitons separated by the typical inter-impurity distance, R_0 .

Because of the small probability of the electron tunneling over the rather large distances involved in the hopping, free-soliton conduction will always dominate at high enough temperatures. However, as the temperature is lowered, the energetics become increasingly important, until eventually hopping dominates. This is reflected in the relatively slow temperature dependence of Eq. (2) when compared with the exponential temperature dependence of Eq. (1). The hopping process is also responsible for the three-dimensional component of the spin diffusion.

The plan of the paper is as follows: In Sec. II, a simple phenomenological reduced Hamiltonian is derived which describes the soliton-impurity system, and a formal expression for the hopping rate between a pair of solitons is obtained. This rate is then used to obtain expressions for the hopping contribution to the various transport coefficients. In Sec. III, a generalized version of the microscop-

ic model Hamiltonian of SSH is taken to represent $(\text{CH})_x$, so that the parameters which enter the reduced Hamiltonian can be evaluated. The assumed values of physical quantities are those listed in Table I. Thus, the transport coefficients are ultimately calculated from a microscopic model of $(\text{CH})_x$. Section IV contains a brief discussion of the free-soliton contribution to the same transport coefficients. In Sec. V, the theoretical results are compared with the results of existing experiments, and predictions are made concerning possible future experiments. In Sec. VI, some considerations that are absent from the present model are discussed briefly. Chief among these is the effects of electron-electron and soliton-soliton interactions which will not be considered until this point. Because of the large number of symbols, the most important symbols that occur throughout this paper are listed in Table I.

II. GENERAL CONSIDERATIONS

In this section, the formal manipulations required to calculate the transport coefficients of interest are discussed. As the considerations are quite general, no detailed model of polyacetylene is adopted. All that is assumed is the existence of solitons of the general nature described in the Introduction and the presence of disorder which is represented as an impurity potential, V_{imp} . In Sec. II A, the hopping rate between a pair of solitons is derived. Then in Sec. II B, the rate equation for hopping transport is reviewed briefly, and expressions for the conductivity and thermopower are derived in terms of the average hopping rates. The theory of multiphonon transitions between localized states has been discussed extensively in the literature,¹⁹ so those steps in the derivation that are similar to the case of hopping between impurities have been omitted. However, there are two aspects of the soliton problem that are not present in the impurity problem. The first is that the soliton is a complicated collective excitation which involves a distortion of the full many-electron wave function and a classical lattice distortion. Thus, the transition rate of interest does not simply involve a change in the state of one electron. The second complication involves the presence of the Goldstone mode associated with the translational motion of the soliton. This mode must be treated on a separate footing from the rest of the phonon modes by defining a collective coordinate which

specifies the position of the soliton.²⁰ Despite these complications, we find that for small soliton effective mass [as in $(\text{CH})_x$], the present hopping problem is equivalent to hopping between impurities with a spectrum of bound states. Finally, we conclude the section by obtaining a criterion for determining whether one-dimensional (intrachain) or three-dimensional (interchain) hopping is dominant.

A. The two-soliton problem

A collection of polyacetylene chains and impurities can be represented by the Hamiltonian

$$H = H_e(\{\vec{R}\}) + V_{\text{imp}} + U(\{\vec{R}\}) + \sum_{nl} \frac{P_{nl}^2}{2M}, \quad (3)$$

where H_e is the electronic Hamiltonian of the pure system which depends parametrically on the set of ionic coordinate $\{\vec{R}\}$, V_{imp} is the potential due to the impurities, U is the ionic potential energy (which includes the effects of the σ electrons), \vec{P}_{nl} is the momentum of the n th C-H group on the l th chain, and M is the C-H mass. The system is constrained to have a soliton on two of the chains, which will be arbitrarily labeled 1 and 2.

To begin with, consider the case in which both solitons are negatively charged (doubly occupied). This situation can be treated accurately within the Born-Oppenheimer approximation, hence the electronic and ionic wave functions can be factored. Excitations of the electronic system, such as the promotion of an electron to the conduction band or the creation of a soliton-antisoliton pair all require

energies in excess of Δ_0 and so are unimportant at all relevant temperatures. The electronic ground state $|\psi\rangle$ will eventually serve as an effective vacuum state. The vibrational states can be expressed in terms of the phonon creation operators b_α^\dagger by expanding the ionic potential energy

$$\begin{aligned} \tilde{U}(\{\vec{R}\}) = & \langle \psi | [H_e(\{\vec{R}\}) + V_{\text{imp}}] | \psi \rangle \\ & + U(\{\vec{R}\}) \end{aligned} \quad (4)$$

to second order in displacement about $\{\vec{R}^{(0)}\}$, the minimum energy configuration is

$$\left[\tilde{U}(\{\vec{R}\}) + \sum_{nl} \frac{P_{nl}^2}{2M} \right] = \sum_{\alpha} \hbar\omega_{\alpha} (b_{\alpha}^{\dagger} b_{\alpha} + \frac{1}{2}). \quad (5)$$

Here α represents an appropriate set of quantum numbers.

When an electron is removed from the system there are two electron states that are important at reasonable temperatures: those in which the negative charge (extra electron) is predominantly on soliton 1, χ_1 , or on soliton 2, χ_2 . Hence, we need only consider matrix elements of the Hamiltonian in a reduced Hilbert space spanned by the direct product states $\{\chi_i \phi_{iA}\}$, where the electronic state vectors χ_i depend implicitly on $\{\vec{R}\}$:

$$\begin{aligned} [H_e(\{\vec{R}\}) + V_{\text{imp}}] \chi_i(\{\vec{R}\}) \\ = \mathcal{E}_i(\{\vec{R}\}) \chi_i(\{\vec{R}\}) \quad \text{for } i=1,2 \end{aligned} \quad (6)$$

and $\phi_{iA}(\{\vec{R}\})$ is a vibrational eigenstate. If we first separate out the translational mode for special treatment, the Hamiltonian can be expanded to in powers of \sqrt{m}/M . To first order, the resulting reduced Hamiltonian is

$$\begin{aligned} H^{(\text{red})} = & \sum_{i=1}^2 \left[\mathcal{E}_i^{(0)} + \sum_{\alpha} \Lambda_{\alpha}^{(i)} \hbar\omega_{\alpha} (b_{\alpha}^{\dagger} + b_{\alpha}) \right] a_i^{\dagger} a_i + \sum_{i=1}^2 [V_{\text{imp}}(X_i) a_i^{\dagger} a_i + T(\dot{X}_i)] \\ & + \sum_{\alpha} \hbar\omega_{\alpha} \lambda_{\alpha} (b_{\alpha}^{\dagger} - b_{\alpha}) (a_1^{\dagger} a_2 - a_2^{\dagger} a_1) + \sum_{\alpha} \hbar\omega_{\alpha} (b_{\alpha}^{\dagger} b_{\alpha} + \frac{1}{2}), \end{aligned} \quad (7)$$

where \sum_{α}' is the sum over the same phonon modes as in Eq. (6) excluding the soliton translational modes, $V_{\text{imp}}(X_i)$ is the electrostatic potential energy of interaction between the soliton i (at position X_i) and the impurity to which it is bound, T is the soliton kinetic energy, and a_i^{\dagger} is the electron creation operator defined by the relation

$$\langle nl | a_i^{\dagger} | \psi \rangle^{(0)} = (\chi_i^{(0)})_{nl}. \quad (8)$$

The dimensionless electron-phonon coupling constants, γ and λ , are both of order $\sqrt{m_e}/M$ and can be calculated in terms of the phonon wave functions, $\vec{\phi}_{\alpha}(nl)$, according to the relations

$$\Lambda_{\alpha}^{(i)} = \frac{1}{\omega_{\alpha} \sqrt{2M \hbar \omega_{\alpha}}} \sum_{nl} \vec{\phi}_{\alpha}(nl) \cdot (\vec{\nabla}_{nl} \mathcal{E}_i)^{(0)}, \quad (9)$$

and

$$\lambda_\alpha = \frac{\hbar}{\sqrt{2M\hbar\omega_\alpha}} \sum_{nl} \vec{\phi}_\alpha(nl) \cdot [\chi_1^\dagger(\{\vec{R}^{(0)}\}) \times \vec{v}_{nl}^{(0)} \chi_2(\{\vec{R}^{(0)}\})] . \quad (10)$$

Since the translational mode is antisymmetric, Eq. (9) gives a zero-linear electron-phonon coupling when α is a translational mode. It is important to note here that $\Lambda_\alpha^{(i)}$ is anomalously small. In the absence of an impurity potential, the system (as described by the SSH Hamiltonian) has particle-hole or charge-conjugation symmetry, thus constraining the midgap state to lie at zero energy independent of the value of the phonon coordinates. Thus, for an unpinned soliton, $\Lambda_\alpha^{(i)} = 0$. The only reason that Λ is nonzero at all is that the impurity potential breaks the charge conjugation symmetry. Nonetheless, we expect Λ to be small. Indeed, SSH have estimated the change, E_p , in the binding energy, E_b , to a charged impurity of an oppositely charged soliton due to its change in width and they found that E_p is less than 10% of E_b [see SSH following Eq. (5.5)]. In Appendix C we show that for $E_p \ll E_b$, multiphonon processes do not affect the phonon-assisted hopping rate dramatically, other than to smooth out any sharp features that might otherwise be present. Thus, in the following discussion we will set $\Lambda = 0$ and thus only consider explicitly single-phonon processes.

We are now in the position to calculate the transition rate, ν , from Fermi's golden rule. The transition rate must be thermally averaged over initial states and summed over final states. The result is of the form

$$\nu = \int d\epsilon_1 d\epsilon_2 \nu_{12}(\epsilon_2 - \epsilon_1) p_1(\epsilon_1) \bar{p}_2(\epsilon_2) . \quad (11)$$

$\nu_{12}(\epsilon - \epsilon_2)$ is the transition rate that would result in the absence of the translational modes (see Appendix C). $p_i(E)$ in Eq. (11) is the probability that when soliton i makes a transition from an initially charged state to the neutral state, it will give up energy ϵ (could be negative) in the transition

$$p_i(\epsilon) = \sum_{\phi_{ch}\phi_n} \frac{e^{-E_{ch}/k_B T}}{Z_{ch}} |\langle \phi_{ch} | \phi_n \rangle|^2 \times \delta(E_{ch} - E_n - \epsilon) , \quad (12)$$

where

$$Z_{ch} = \sum_{\phi_{ch}} e^{-E_{ch}/k_B T} \quad (13)$$

and $|\phi_{ch}\rangle$ ($|\phi_n\rangle$) is a translational eigenstate of the charged (neutral) soliton with energy E_{ch} (E_n) (note these energies include the potential energy of interaction between the soliton and the impurity as well as the soliton's kinetic energy.) $\bar{p}_i(\epsilon)$ is the probability that the soliton translational mode will absorb energy ϵ in the reverse process

$$\bar{p}_i(\epsilon) = \sum_{\phi_{ch}\phi_n} \frac{e^{-E_n/k_B T}}{Z_n} |\langle \phi_n | \phi_{ch} \rangle|^2 \times \delta(E_n - E_{ch} - \epsilon) , \quad (14)$$

where

$$Z_n = \sum_{\phi_n} e^{-E_n/k_B T} . \quad (15)$$

In Sec. III, it is shown that the kinetic energy of the neutral soliton is small. If E_n can be neglected,²¹ the expressions for $p_i(\epsilon)$ and $\bar{p}_i(\epsilon)$ can be simplified and their physical interpretation becomes transparent:

$$p_i(\epsilon) = \frac{\rho_i(\epsilon) e^{-\epsilon/k_B T}}{Z(T)} \quad (16)$$

and

$$\bar{p}_i(\epsilon) = \frac{\rho_i(\epsilon)}{Z(\infty)} , \quad (17)$$

where $\rho_i(\epsilon)$ is the density of states of the charged soliton,

$$\rho_i(\epsilon) = \sum_{\phi_{ch}} \delta(\epsilon - E_{ch}) , \quad (18)$$

and $Z(T)$ is the corresponding partition function [$Z(\infty) = N$, the number of carbons per chain]. Thus, if soliton 1 is initially charged, $p_1(\epsilon)$ ($\bar{p}_2(\epsilon)$) is the probability that the initial (final) state of soliton 1 (2) has energy ϵ .

The ϵ_2 integral in Eq. (11) and the phonon-state summations implicit in ν_{12} can be performed to yield the expression

$$\nu = \int d\epsilon p_1(\epsilon) \int_0^\infty dE g(E) E^2 \{ \bar{p}_2(\epsilon - E) [1 + n(E)] + \bar{p}_2(\epsilon + E) n(E) + O(\bar{p}'_2(E) E_p) \} , \quad (19)$$

where $g(E)$ is the effective electron-phonon coupling

$$g(E) = \sum_{\alpha} \lambda_{\alpha}^2 \delta(E - \hbar\omega_{\alpha}), \quad (20)$$

and $n(E) = (e^{-E/k_B T} + 1)^{-1}$ is the Bose occupation number.

To complete the formal derivation of the transition rate, the dependence of λ_{α} on the separation, \vec{R} , between solitons must be discussed. The method of Miller and Abrahams¹⁹ (MA) is employed. Thus, we expand the electronic states $|i\rangle$ in terms of the states $|S_i\rangle$, where $|S_i\rangle$ is the bound-state wave function in the presence of a single soliton $|i\rangle$. We define the parameter

$$g = \frac{\langle S_1 | H_e | S \rangle}{(\epsilon_1 - \epsilon_2)} \equiv \frac{I_0 \mathcal{S}}{(\epsilon_1 - \epsilon_2)}, \quad (23)$$

and the overlap matrix

$$\mathcal{S} = \langle S_1 | S_2 \rangle. \quad (24)$$

In general, we are also interested in the case $I_0 \gg |\epsilon_1 - \epsilon_2|$ [see Eq. (23)], since I_0 is typically of order of a few electron volts and $|\epsilon_1 - \epsilon_2|$ for states of interest is of order $k_B T$. In this limit it is easily shown by the method of MA that

$$\lambda_{\alpha} \approx \frac{1}{(\epsilon_1 - \epsilon_2)} \sum_{nl} \frac{\vec{\phi}_{\alpha}(nl) \cdot \hbar \vec{\nabla}_{nl} \langle S_1 | H_e | S_2 \rangle}{\sqrt{2M \hbar \omega_{\alpha}}}. \quad (25)$$

From this it is apparent that the transition rate is proportional to the square of the electronic overlap \mathcal{S} which dominates the position dependence of ν_{12} . \mathcal{S} generally depends exponentially on R , so we will assume

$$\mathcal{S}(R) \approx \exp\{ -[(R_{\parallel}/\xi_{\parallel})^2 + (R_{\perp}/\xi_{\perp})^2]^{1/2} \}, \quad (26)$$

where R_{\parallel} is the component of R along the chain direction, and R_{\perp} is the distance perpendicular to the chain. Equation (27) reflects the anisotropic effective-mass characteristic of a quasi-one-dimensional system. To simplify the percolation analysis in Sec. II B, it is convenient to express ν_{12} as a product of an R -dependent overlap and an R -independent part,

$$\nu \equiv \mathcal{S}^2(R) \gamma(T) (1/N), \quad (27)$$

where the factor $1/N$ in the definition of $\gamma(T)$ reflects the probability that the neutral soliton is near an impurity.

B. Rate equation

In this section expressions are derived for the conductivity and the thermopower in terms of the average two-site hopping rate in Eq. (27). The method of Ambegaokar, Halperin, and Langer²² (AHL) is employed to convert the hopping problem to that on an equivalent resistor network.

Consider a simple model system consisting of equivalent sites i , each of which can be either unoccupied or occupied by a single electron. In addition, however, suppose that at each site the electron can occupy one of many states. These sites, which we identify with the impurities in Sec. II A, are assumed to be randomly distributed with a mean concentration c_{imp} . The average transition rate from site i to site j is

$$\Gamma_{ij} = \langle n_i (1 - n_j) \rangle \nu_{ij}, \quad (29)$$

where n_i is the occupation number of site i and ν_{ij} is a transition rate that is independent of the site-occupation probability. In thermal equilibrium,

$$\langle n_i (1 - n_j) \rangle = \langle n_i \rangle \langle (1 - n_j) \rangle.$$

As in Eq. (14), ν_{ij} is the average transition rate from states on site i to states on site j :

$$\begin{aligned} \nu_{ij} = & \int d\epsilon_i d\epsilon_j \frac{e^{-\epsilon_i/k_B T}}{Z(T)} \\ & \times \rho(\epsilon_i) \frac{\rho(\epsilon_j)}{Z(\infty)} \nu_{ij}(\epsilon_i, \epsilon_j), \end{aligned} \quad (30)$$

where $\nu_{ij}(\epsilon_i, \epsilon_j)$ is the transition rate from the state of energy ϵ_i on site i , to the state of energy ϵ_j on site j , and $\rho(\epsilon)$ is the density of states on a given site. The condition of detailed balance requires that, in thermal equilibrium,

$$\Gamma_{ij}^{(0)} = n^{(0)} (1 - n^{(0)}) \nu_{ij} = \Gamma_{ji}^{(0)}, \quad (31)$$

where $\Gamma_{ij}^{(0)}$ is the average flux from i to j in equilibrium and

$$n^{(0)} = 1 / \{ 1 + \exp[-\mu/k_B T - \ln Z(T)] \},$$

is the fraction of occupied sites.

Following AHL, we introduce a weak electric field which perturbs the site energies,

$$\epsilon_i \rightarrow \epsilon_i + e \vec{\mathcal{E}} \cdot \vec{R}_i,$$

and, consequently, the local chemical potential,

$\mu_i = \mu + \delta\mu_i$, must be allowed to vary to insure current conservation. In addition we suppose, following Emin,²³ that it is possible to define a local temperature which varies slowly across the sample,

so that the temperature at site i is $T_i = T + \delta T_i$. The net flow from site i to site j can then be calculated in a manner exactly analogous to the AHL equation (4.3) and the Emin equation (3):

$$\Gamma_{ij} - \Gamma_{ji} = \frac{1}{k_B T} \Gamma_{ij}^{(0)} \left[e^{\vec{\mathcal{E}} \cdot (\vec{R}_i - \vec{R}_j)} + \delta\mu_i - \delta\mu_j + k_B (\delta T_i - \delta T_j) T \frac{\partial \ln(\Gamma_{ij}/\Gamma_{ji})}{\partial T_i} \Big|_{T_i=T_j=T} \right]. \quad (32)$$

As in AHL, the first two terms in the large parentheses are the potential difference between sites i and j , so the quantity

$$G_{ij} = e^2 \Gamma_{ij}^{(0)} / k_B T$$

can be interpreted as a conductance. In addition to the potential difference, there is a term proportional to the temperature gradient. To evaluate the coefficient of this term, the derivative of Γ_{ij} with respect to the local temperatures T_i and T_j must be computed. $\nu_{ij}(\epsilon_i, \epsilon_j)$ in the expression for Γ_{ij} in Eq. (32) is the quantum-mechanical transition rate for an electron in a state with energy ϵ_i on site i to a state with energy ϵ_j on site j . Thus, it contains a complicated temperature dependence through the Bose occupation factors, as can be seen explicitly in Eq. (30). However, because the phonon absorption or emission that accompanies the transition is just as likely to occur in the vicinity of site i as in the vicinity of site j ,

$$\frac{d\nu_{ij}(\epsilon_i, \epsilon_j)}{dT_i} \Big|_{T_i=T_j=T} = \frac{d\nu_{ji}(\epsilon_i, \epsilon_j)}{\partial T_j} \Big|_{T_i=T_j=T}, \quad (33)$$

and therefore

$$\frac{T \partial \ln(\Gamma_{ij}/\Gamma_{ji})}{\partial T_i} \Big|_{T_i=T_j=T} = \left[\bar{\epsilon}_{ij} + k_B T \ln \left(\frac{n^{(0)}}{1-n^{(0)}} \right) + k_B T \ln Z(T) \right], \quad (34a)$$

where $\bar{\epsilon}_{ij}$ is the average energy transported per hop:

$$\bar{\epsilon}_{ij} \equiv \nu_{ij}^{-1} \int d\epsilon_i d\epsilon_j \epsilon_i \frac{\rho(\epsilon_i) e^{-\epsilon_i/k_B T}}{Z(T)} \frac{\rho(\epsilon_j)}{Z(\infty)} \nu_{ij}(\epsilon_i, \epsilon_j). \quad (34b)$$

If the average transition rate ν_{ij} can be factored into an R -dependent overlap factor and an R -independent factor as in Eq. (28), the conductivity and thermopower can be calculated separately. The thermopower is especially simple, since $\bar{\epsilon}_{ij} = \bar{\epsilon}$, independent of i and j , so

$$S = \frac{e}{k_B} \{ \bar{\epsilon} / k_B T + \ln[n^{(0)} / (1-n^{(0)})] + \ln Z(T) \}. \quad (35)$$

If, in addition, the electronic overlap factor takes the simple form described in Eq. (26), the dc conductivity is that of the so-called R -percolation problem.²⁴ An approximate analytic formula for the conductivity can be obtained by the method of Butcher *et al.*,²⁵ as described in Appendix A. This approximation scheme has been found to yield results in good quantitative agreement with results of computer simulation experiments, and so can be used with some degree of confidence. Thus, if R_0 is the typical separation between impurities (sites in the model problem),

$$R_0 = (4\pi c_{\text{imp}}/3)^{-1/3}, \quad (36)$$

and ξ is the three-dimensionally averaged electronic decay length

$$\xi = (\xi_{\parallel} \xi_{\perp}^2)^{1/3}, \quad (37)$$

then,

$$\sigma = Ae^2 \frac{n^{(0)}(1-n^{(0)})}{k_B T} \frac{\gamma(T)}{N} \left[\frac{\xi}{R_0^2} \right] e^{-2BR_0/\xi} \left[1 + O \left(\frac{\xi}{R_0} \right) \right], \quad (38)$$

where $A = 0.45$ and $B = 1.39$. To relate σ in Eq. (38) to the conductivity of polyacetylene, $n^{(0)}$ is interpreted as the fraction of solitons that are charged and $1 - n^{(0)}$ the fraction that are neutral¹⁷ [see Eq. (2)]. Because of the large-scale topological disorder of polyacetylene, a single isotropic conductivity is quoted in Eq. (38). In a single crystal, a relatively small anisotropy, $\sigma_{\perp}/\sigma_{\parallel} = (\xi_{\perp}/\xi_{\parallel})^2$, would be observed where σ_{\parallel} (σ_{\perp}) is the conductivity in the in-chain (out-of-chain) direction. The isotropic conductivity observed in actual polyacetylene is the average over angles of σ_{\perp} and σ_{\parallel} , $\sigma = \frac{1}{3}(\sigma_{\parallel} + 2\sigma_{\perp})$.

Two aspects of the above discussion warrant closer attention. The first is the assumption that all sites are equivalent. This assumption allowed us to calculate the thermopower from the averaged properties of the hop between a single pair of sites, without considering the percolation aspects of the problem which determine the conductivity. In the presence of multiple flavors of sites, that is sites possessing a variety of spectra, $\rho_i(\epsilon)$, the expression for the thermopower must be averaged in a complicated way over all possible pairs of sites. In the case of hopping between solitons, we in fact expect a variety in "site" characteristics due to a distribution of impurity-chain spacings, β . However, differences of up to a half an angstrom produce only hundredths of volts changes in E_b (SSH estimate $E_b = 0.3$ eV for $\beta = 2.4$ Å, and $E_b = 0.32$ eV for $\beta = 2.0$ Å, and still smaller changes in ω_1 .) Since Eq. (35) depends only logarithmically on the two-site transition rates, a distribution of soliton binding energies of width δE_b will make, *at most*, a contribution

$$\delta S \sim e/k_B (\delta E_b/k_B T)$$

to the thermopower. At the temperatures of interest, this is small compared to the result in Eq. (35). A variety in "site" characteristics can also result from soliton-soliton and electron-electron interactions. The discussion of this effect will be postponed to Sec. V.

The second aspect is the assumed three-dimensional (3D) nature of the hopping problem. In computing the conductivity in Eq. (38), the quasi-one-dimensional nature of the system was included

only in the anisotropy of the effective mass which leads to the anisotropic electronic overlap factor described in Eq. (26). The discrete nature of the polyacetylene chains has been ignored. This approximation is valid so long as the typical interchain hopping rate, ν_{3D} , is much greater than the typical intrachain hopping rate, ν_{1D} . To test the validity of this assumption, consider the typical 1D and 3D hops:

$$\ln \nu_{3D} \sim \ln \gamma - 2R_0/\xi, \quad (39)$$

where R_0 is the typical separation between impurities given in Eq. (36), and ξ is a dimensionally averaged decay length [see Eq. (37)] which must clearly be in the range $\xi_{\parallel} > \xi > \xi_{\perp}$ on physical grounds alone. Similarly,

$$\nu_{1D} \sim \ln \gamma - 2R_1/\xi_{\parallel}, \quad (40)$$

where R_1 is the typical separation between impurity sites on a given chain

$$R_1 \sim (b^2 c_{\text{imp}})^{-1}, \quad (41)$$

where b is the interchain separation. The linear dependence of R_1 on c_{imp}^{-1} as opposed to the one third power dependence of R_0 , implies that interchain hopping always dominates intrachain hopping at low impurity concentrations. In Appendix B it is shown that the fraction of sites which have $\nu_{1D} > \nu_{3D}$ is

$$\left(\frac{3}{\pi} \right)^{1/2} \left| \frac{\xi_{\parallel}}{\xi_{\perp}} \right| c_{\text{imp}} b^3 + O(c_{\text{imp}}^2).$$

This is much less than one at all the dopant concentrations considered in this paper. Notice, however, that the conduction becomes increasingly one dimensional as the dopant concentration is *increased*.

Finally, formal expressions for the ac conductivity $\sigma(\omega)$, the Hall mobility μ_H , and the hopping contribution to the spin-diffusion constant D_{hop} can be derived readily.

The ac hopping conductivity in a disordered system is always much larger than the dc conductivity. Physically, this is due to the presence of pairs or larger clusters of anomalously close sites between which an electron can hop at a rate far

greater than the rate which characterizes the difficult hops on the percolation network. So long as the photon energy $\hbar\omega$ is small compared to $k_B T$, the ac conductivity, like the dc conductivity, is equivalent to that of an R -percolation network. (At higher frequencies, photon-assisted hopping be-

comes important.) The pair approximation, which yields results in good agreement with numerical simulation experiments,²⁶ provides an approximate analytic expression for the excess conductivity:

$$\sigma(\omega) - \sigma_{dc} = -\frac{\omega e^2 c_{imp}^2}{6k_B T N} \int \frac{R^2 d\vec{R} \mathcal{S}(\vec{R}) n^{(0)}(1-n^{(0)})}{[\omega/\Gamma_0 + 2i\mathcal{S}(\vec{R})]} \approx \frac{e^2}{\hbar} \frac{(c_{imp})^2}{(k_B T)} \frac{n^{(0)}(1-n^{(0)})}{12} \frac{\xi_{||}^3 \xi_{\perp}^2}{2^5} \hbar\omega [\ln(2\omega/\Gamma_0)]^4, \quad (42)$$

where $\Gamma_0 = n_0(1-n_0)\gamma/N$.

An expression for the Hall mobility was obtained by Friedman and Pollak,²⁷ but it is expected to be very small in the present system.

To obtain an expression for the conductivity, we expanded the transition rates in Eq. (34) to first order in $e\vec{\mathcal{E}} \cdot (\vec{R}_i - \vec{R}_j)/k_B T$. Therefore, non-Ohmic effects are expected to become apparent for electric fields greater than \mathcal{E}_0 :

$$\mathcal{E}_0 = k_B T / (eR_{char}), \quad (43)$$

where R_{char} is the longest characteristic hopping distance on the percolation path. The same considerations that led to Eq. (38), yield an expression for R_{char} :

$$R_{char} = (\xi_{||}/\xi) BR_0. \quad (44)$$

The details of the electric-field dependence in the non-Ohmic regime are complicated and will be considered in a future publication.

Since the spin is transported at each hop (although in the opposite direction to the charge transport) the hopping contribution to the spin-diffusion constant is related to the hopping conductivity by the Einstein relation,

$$D_{hop}(\omega) = \left[\frac{1}{e^2} \right] \frac{k_B T}{c_{imp}} \sigma(\omega). \quad (45)$$

Notice that the present contribution to the spin-diffusion constant is small (because σ is small) and intrinsically three dimensional. It will certainly be masked by the one-dimensional free-soliton spin diffusion at all but the lowest frequencies.

III. THE MAGNITUDE OF THE CONDUCTIVITY: THE SSH MODEL

At this point it remains only to evaluate the general formulae derived in the last section for the electronic transition rate between a pair of soliton bound states using a microscopic model of polyacetylene. There are two major stumbling blocks. Firstly, the SSH model of polyacetylene, which is the most successful microscopic model to date, is a purely one-dimensional model. To calculate a three-dimensional property, such as the hopping rate, it is necessary to construct a three-dimensional model. Secondly, even for a single strand of polyacetylene, the phonon wave functions which enter Eqs. (9) and (10) are not known. (Calculations of Mele and Rice²⁸ promise to alleviate this difficulty in the near future.) Thus, the electron-phonon coupling constants can only be estimated.

Given this state of affairs, it is tempting to adopt an empirical form for the transition rate $\gamma(T)$ [defined in Eq. (21)] and to assume "reasonable" values for the electronic decay lengths, $\xi_{||}$ and ξ_{\perp} [defined in Eq. (26)]. For instance, if we assume that

$$\gamma(T) = \gamma_0 (T/T_0)^x,$$

a good fit is obtained to the experimentally observed conductivity and thermopower for a suitable choice of the values of the parameters. However, it is important to ascertain whether these are reasonable values. It is, *a priori*, possible that the actual hopping rates are too small to account for the observed conductivity at reasonable temperatures. If this were the case, we would have to conclude that hopping is only important at ultralow temperatures and that the agreement with experiment is fortuitous.

In this section, therefore, we adopt a simple three-dimensional generalization of the SSH model, and use it to estimate the magnitude and temperature dependence of the various transport properties of $(\text{CH})_x$. Given the rudimentary nature of our knowledge of the interactions between chains, these interactions are included in the simplest possible fashion. Specifically, the quantities to be evaluated are the soliton energy-distribution functions $p_i(\epsilon)$ and $\bar{p}_i(\epsilon)$ [defined in Eqs. (12)–(16)], and the electron-phonon coupling function $g(E)$ [defined in Eq. (20)]. The first two quantities are basically²¹ properties of the soliton-bearing chain, and hence can be estimated using only the (one-dimensional) SSH model. $g(E)$ is intrinsically three dimensional as it is proportional to the electronic overlap.

The SSH Hamiltonian is a simple, tight-binding Hamiltonian which represents a single strand of polyacetylene in the absence of impurities as a linear chain of carbons with one π orbital per carbon (with creation operator c_n^\dagger) coupled to one ionic degree of freedom per carbon, the dimerization or in-chain displacement u_n :

$$H_{\text{SSH}} = \sum_n [t_0 + \alpha(u_{n+1} - u_n)](c_{n+1}^\dagger c_n + c_n^\dagger c_{n+1}) + \frac{K}{2} \sum_n (u_{n+1} - u_n)^2. \quad (46)$$

Values appropriate to polyacetylene of the various constants which appear in Eq. (46) are listed in Table I. The properties of H_{SSH} have been explored in detail by SSH within a mean-field, Born-Oppenheimer approximation, so only those results that are necessary for the present calculations are discussed here.

According to the SSH equation (4.14), the pattern of lattice displacements associated with a soliton which minimizes the potential energy is

$$u_n = u_0 (-1)^n \tanh(n/l_{||}), \quad (47)$$

where $l_{||} \equiv (\xi_{||}/a) \approx 2t_0/\Delta_0$ and $|u_0|$ is the magnitude of the equilibrium dimerization $|u_0| = \Delta_0/4\alpha$. Midgap states (such as the soliton bound state) are generally expressible as a slowly varying envelope function times a gap-edge Bloch state with $k = \pi/2a$. In particular, according to the SSH equation (4.21), the Hamiltonian can always be diagonalized by the state (normalizable only in the presence of a soliton):

$$\begin{aligned} \chi(2+n) &= (-1) \left[\frac{t_0 + \alpha(u_{2+n-1} - u_{2+n-2})}{t_0 + \alpha(u_{2+n} - u_{2+n-1})} \right] \chi(n) \\ &\approx -[\chi' \cos(\pi/2n) + \chi'' \sin(\pi/2)] \left[\exp \left[-2\alpha/t_0 \sum_{m=0}^{n+2} (-1)^m u_m \right] + O \left[\frac{\alpha^2 u^2}{t_0^2} \right] \right], \end{aligned} \quad (48)$$

where $\chi(n)$ is the amplitude of the wave function on site n , and χ' and χ'' are constants. The spatial decay of the wave function along a chain is determined by the "local" value of the band gap, $8\alpha(-1)^m u_m$. Quantities such as the soliton effective mass m^* and the energy of interaction between a charged soliton and an impurity have also been calculated from this model Hamiltonian by SSH.

$p_i(\epsilon)$ and $\bar{p}_i(\epsilon)$ are measures of the distribution of soliton translational energies. Ignoring "relativistic" corrections, the maximum kinetic energy of a neutral soliton is estimated to be $\frac{1}{2}m^*c^2 = 0.0009$ eV, where c is the speed of sound. "Relativistic" corrections may increase this energy, but probably at most a factor of $(\xi_0/a)^2$.²⁹ The soliton kinetic energy is always small compared to E_b . Thus, $p_i(\epsilon)$ and $\bar{p}_i(\epsilon)$ can be related to a smoothed density of states $\rho(\epsilon)$ of the charged soliton as in Eq. (16). At low energies, the potential energy associated with the impurity-soliton interaction is

harmonic, so

$$\rho(\epsilon) \approx \frac{\Theta(E_b + \epsilon)}{\hbar\omega_1},$$

where $\hbar\omega_1$ is the quantum of soliton vibrational energy. SSH estimate $\hbar\omega_1 = 0.06$ eV [SSH, Eq. (5.5)]. At higher energies, the solitons become essentially free, which results in a large density of states with energy approximately equal to zero. The total number of states $Z(\infty)$ must equal the number of carbon atoms on the chain N . For $N \gg (E_b/\hbar\omega_1)$ the density of states can be roughly approximated by the expression

$$\rho(\epsilon) \approx \frac{\Theta(E_b + \epsilon)\Theta(-\epsilon)}{\hbar\omega_1} + N\delta(\epsilon). \quad (49)$$

To calculate $g(E)$, a three-dimensional generalization of the SSH model must be considered. To this end, we label the atoms with a pair of indices,

l and n , signifying the n th carbon on chain l . In addition to the in-chain interactions, which we assume to be well described by H_{SSH} , a simple electronic interchain coupling is included of the form

$$H_{3D} = t_1 \sum_{\langle l,l' \rangle} \sum_n (c_{ln}^\dagger c_{l'n} + \text{H.c.}), \quad (50)$$

where the $\langle l,l' \rangle$ sum is over nearest-neighbor chains. We assume that t_1 is sufficiently small that all one-dimensional properties, such as the lattice dynamics and the nature of the solitons, are substantially the same as in the absence of H_{3D} (see discussion in Sec. VI). The effect of H_{3D} is assumed to be reflected *solely* in the three-dimensional nature of the electronic wave functions, in

$$\chi(n,l) \approx [\chi' \cos(n\pi/2) + \chi'' \sin(n\pi/2)] \exp \left\{ - \left[\frac{l^2}{l_1^2} + \left(2\alpha/t_0 \sum_{m=0}^n (-1)^m u_m \right)^2 \right]^{1/2} \right\}, \quad (51)$$

where $\chi(n,l)$ is the amplitude on the carbon n,l of the bound-state wave function of a soliton at the origin. Here $l_1 = \xi_1/b$, where ξ_1 is the decay length of the wave function perpendicular to the chain and b is the interchain separation. Thus, the one relevant parameter which depends on H_{3d} is ξ_1 . In Appendix B an expression is obtained for the wave function of a midgap (zero-energy) state of a perfectly dimerized [$u_{nl} = (-1)^n u_0$] array of chains. For $t_1 \ll \Delta_0$, the wave function falls off exponentially with l according to the expression

$$\chi(0,l) \sim \left[\frac{t_1}{\Delta_0} \right]^l \quad (52)$$

and for large l ,

$$\xi_1 = b / \ln(\Delta_0/t_1) \approx 2.3 \text{ \AA}.$$

Equation (52) can be readily understood by considering H_{3d} as a perturbation since the bound-state wave function first develops an amplitude on the l th chain in the l th-order perturbation theory. Δ_0 is thus interpreted as the typical energy mismatch between the bound state and the band-edge states on the neighboring chains.

Finally, we must estimate $g(E)$. Rather than attempting to evaluate this function in detail, which would require explicit forms for all the phonon wave functions, we will assume that $g(E)$ is a simple, smooth, single-peaked function of energy;

$$g(E) \propto E^x e^{-E/E_0}. \quad (53)$$

particular of the soliton bound states. Although even here, the effect of H_{3D} is relatively small, it is essential since in its absence there is *no* overlap between soliton bound states on different chains.

Consider the bound state of a soliton at the origin ($l=0, n=0$). As in the one-dimensional case, Eq. (48), the wave function is expressible as a slowly varying function times a gap-edge Bloch state. The envelope function is expected to be of the same general form as that of a bound state in a three-dimensional continuum with an anisotropic effective mass [Eq. (27)], which we combine with the expression in Eq. (48) for the in-chain decay as a function of lattice displacement. The result is

$g(E)$ can then be characterized by a magnitude [the proportionality constant in Eq. (53)], a peak energy $x E_0$, and a peak half-width $\sqrt{x} E$. While the exact $g(E)$ probably has more structure, the insights obtained into the behavior of $g(E)$ are expected to survive a more painstaking analysis. We will calculate the magnitude of $g(E)$ from the sum rule:

$$\int E g(E) dE = \frac{\hbar^2}{2M} \sum_{nl} \frac{|\vec{\nabla}_{nl} \langle S_1 | H_e | S_2 \rangle|^2}{(\epsilon_1 - \epsilon_2)^2}, \quad (54)$$

which follows from Eq. (25) and the completeness of the phonon wave functions, and is independent of the phonon wave functions. Since the electronic wave functions are known [Eq. (51)], the sum in Eq. (54) can be performed readily:

$$\int g(E) E dE = \frac{\Delta_0^2 \varphi^2}{(\epsilon_1 - \epsilon_2)^2} \left[\frac{\hbar^2}{2mu_0^2} \right] f, \quad (55)$$

where, from the continuum theory, we have taken

$$(\chi_1' \chi_2'' + \chi_1'' \chi_2') = (l_1^2 l_{||} \pi)^{-1}$$

and

$$f = [(R_0/\xi)^2 + 2(R_0/\xi) + 2]/8 \approx 1.$$

To determine the peak position and width of $g(E)$, we consider the form of the electron-phonon coupling λ_α in more detail. Equation (51) can be

used to evaluate Eq. (26) for λ_α :

$$\lambda_\alpha \approx \frac{t_0}{(\epsilon_1 - \epsilon_2)} (\chi'_1 \chi'_2 + \chi'_1 \chi'_2) \left[\frac{2\alpha \hbar}{t_0} \right] \sum_{nl} \frac{(-1)^n \phi_\alpha(nl)}{\sqrt{2M\hbar\omega_\alpha}} \\ \times \exp \left[- \left[\frac{l^2}{l_1^2} + \frac{(n-n_1)^2}{l_{||}^2} \right]^{1/2} - \left[\frac{(l-l_2)^2}{l_1^2} + \frac{(n-n_2)^2}{l_{||}^2} \right]^{1/2} \right].$$

The $(-1)^n$ in the sum implies that the coupling is indeed predominantly to the optical phonons. We therefore conclude that the peak of $g(E)$ falls at an average optical-phonon frequency, $\hbar\omega_0 \approx 0.15$ eV, and that the peak width is determined by the half-width of the optical-phonon spectrum, $\hbar\Delta\omega \approx 0.05$ eV. Thus, the three parameters in $g(E)$ are determined. The resulting function

$$g(E) = \left[\frac{E_1}{\epsilon_1 - \epsilon_2} \right]^2 \frac{\mathcal{J}^2 x^2}{\hbar\omega_0} \left[\frac{tE}{\hbar\omega_0} \right]^x \frac{e^{-(xE/\hbar\omega_0)}}{(x+1)!}, \quad (56)$$

is peaked at $E = \hbar\omega_0$, satisfies the sum rule in Eq. (55) if

$$E_1 = \Delta_0 \left[\left[\frac{\hbar^2}{2Mu_0^2} \right] \left[\frac{1}{\hbar\omega_0} \right] \right]^{1/2} \approx 0.5 \text{ eV},$$

and has a half-width $\Delta\omega$ so long as $x = (\omega_0/\Delta\omega)^2 \approx 9$. The results in Eqs. (49) and (56) can be combined to evaluate $\gamma(T)$ in Eq. (21):

$$\hbar\gamma(T) = \frac{E_1^2}{\hbar\omega_1} \left[\frac{xk_B T}{\hbar\omega_0} \right]^{x+1} \left[\frac{x}{x+1} \right] \left[1 + O \left[\frac{kT}{\hbar\omega_0} \right] \right] \\ \approx 500 \text{ eV} \left[\frac{T}{300 \text{ K}} \right]^{10}. \quad (57)$$

The value of $\gamma(T)$ may seem unduly large as it is often assumed to be roughly of the order of a phonon frequency. A similar phenomenon has been noted,²⁵ for instance, in empirical studies of hopping conduction in *a*-Ge, where a similarly defined frequency is found to be about 3 orders of magnitude larger than a typical phonon frequency. The maximum hopping rate can probably never exceed a typical phonon frequency. However, the actual hopping rate in Eq. (28) is less than $\gamma(T)$ by a factor $\mathcal{J}^2(R)$, and thus does not exceed ω_0 at low enough temperatures and concentrations. Finally, the average energy transported per hop, $\bar{\epsilon}$ in Eq. (34b), which determines the thermopower, can be evaluated:

$$\bar{\epsilon} = k_B T \left[\frac{(x+3)}{2} + O \left[\frac{xk_B T}{\hbar\omega_0} \right] \right].$$

IV. HIGH-TEMPERATURE RESULTS

At high temperatures it is no longer true that all of the charged solitons are bound to impurities. When a significant number of free charged solitons are present, free-soliton conduction dominates hopping conduction because of the smallness of the electron-overlap factors that enter the hopping rates. To determine the temperature T_{hop} at which the transition occurs, the magnitude of the high-temperature process must be calculated. Unfortunately, the free-soliton contribution to the conductivity σ_{sol} depends exponentially on $E_b/k_B T$, and E_b is only known approximately. Thus, a direct first principle estimate of T_{hop} is not possible. Nonetheless, a careful comparison of the high-temperature theory with experiment in lightly doped CH_x ($y \lesssim 0.5\%$) allows us to rule out free-soliton conduction as the dominant conduction mechanism at all temperatures that have been observed experimentally. Using certain assumptions, it also allows us to obtain a new experimental lower bound on E_b which is slightly larger than that obtained by SSH.

The free-soliton contribution to the conductivity σ_{sol} is proportional, through an Einstein relation, to the product of the concentration of free solitons and the free-soliton diffusion constant.

To calculate the concentration of free solitons, we must determine the soliton chemical potential μ . The general dependence of μ on temperature and impurity concentration is moderately insensitive to the details of the soliton-impurity interaction, so we can adopt a simplified model to illustrate the behavior of μ . With each impurity we associate x possible soliton bound states, all with energy $-E_b$ on each of n_c neighboring chains. Because of the large size of the soliton, no more than

one soliton per chain can be bound to a given impurity. There are N possible "free"- (zero-energy) soliton states. Finally, for each impurity introduced into the system, n_s charged solitons are introduced into the system. For this model, the chemical potential is determined by the equation:

$$n_s y = \frac{1}{1 + e^{-\beta\mu}} + \frac{n_c x y}{x + e^{-\beta(E_b + \mu)}}, \quad (58)$$

where y is the impurity concentration, $y = N_i/N$ with N_i equal to the number of impurities, and $\beta = 1/k_B T$. The first term on the right-hand side of Eq. (58) is the concentration of free solitons. At low temperatures

$$T \ll T_0 \equiv E_b/k_B \ln(n_s y)$$

and μ is a discontinuous function of the parameter $n \equiv n_s/n_c$:

$$\mu = \begin{cases} -E_b - k_B T \ln[(1-n)x/n] & \text{for } n < 1 \\ -E_b/2[1 - (T/T_0)] & \text{for } n = 1 \\ -k_B T \ln \left[\frac{1 - (n_s - n_c)y}{(n_s - n_c)y} \right] & \text{for } n > 1. \end{cases} \quad (59)$$

In polyacetylene, it is probable that the $n < 1$ result is appropriate although the possibility exists that electron-electron interactions drive the system to the $n = 1$ limit.³⁰ Thus, both possibilities will be considered here. At high temperatures ($T \gg T_0$)

$$\mu = -E_b(T/T_0) \quad (60)$$

regardless of n . However, T_0 is quite large ($T_0 \sim 500$ K for $y = 0.001$), so we are generally interested in the low-temperature results. The low-temperature conductivity is

$$\sigma_{\text{sol}} = \frac{e^2}{k_B T} c D_{\text{ch}} \times \begin{cases} \left[\frac{1-n}{n} \right] x e^{-E_b/k_B T} & \text{if } n < 1 \\ \left[\frac{y}{n_c} \right]^{1/2} e^{-E_b/2k_B T} & \text{if } n = 1, \end{cases} \quad (61)$$

where D_{ch} is the free-charged-soliton diffusion constant, and c is the density of carbon atoms.

The thermopower is

$$S = \frac{e}{k_B} \times \begin{cases} \frac{E_b}{k_B T} + \ln \left[\frac{(1-n)x}{n} \right] & \text{if } n < 1 \\ \frac{E_b}{2k_B T} + \frac{E_b}{2k_B T_0} & \text{if } n = 1. \end{cases} \quad (62)$$

Note that in both cases, thermopower and conductivity are simply activated. Also note that the concentration of free solitons, and hence the conductivity is independent of the concentration of impurities for $n < 1$ and only weakly dependent³⁰ on it for $n = 1$. Both these properties of free-soliton conduction seem to be incompatible with experiment.

In the ideal SSH model in the absence of disorder, the charged-soliton diffusion constant is equal to the neutral-soliton diffusion constant

$$D_n = D_{\text{ch}}. \quad (63)$$

For the sake of argument, we will assume that this equality persists in real polyacetylene, although many mechanisms³¹ can be envisaged that would invalidate Eq. (63). D_n can be measured directly as it is also the in-chain spin-diffusion constant. So as to obtain an analytic expression for D_n , we will not adopt this empirical value, but rather the low temperature ($k_B T \ll \hbar\omega_0$) formula for the soliton-diffusion constant derived by Schrieffer and Wada³² for a ϕ^4 soliton. The similarity between the ϕ^4 soliton and the solitons in polyacetylene has been exploited by several authors, and the predicted value of the diffusion constant is in reasonable agreement with experiment.¹³ The resulting expression for D_n is:

$$D_n = 0.516 \omega_0 a^2 \left[\frac{k_B T}{M u_0^2 \omega_0^2} \right]^2. \quad (64)$$

Since the free-soliton contribution to the conductivity must be less than or equal to the observed conductivity, a lower bound to E_b can be obtained if D_{ch} is known. If σ_{expt} is the measured value of the conductivity, then

$$E_b/k_B T \geq \begin{cases} \ln(\sigma_0/\sigma_{\text{expt}}) + n \left[\frac{1-n}{n} \right] x & \text{if } n < 1 \\ 2 \ln(\sigma_0/\sigma_{\text{expt}}) + n(y/n_c) & \text{if } n = 1, \end{cases} \quad (65)$$

where $\sigma_0 = 6 \times 10^2 \Omega^{-1} \text{cm}^{-1}$ for $T = 300$ K. For convenience, we consider a reference concentration

of AsF_5 , $y=0.003$, and a reference temperature of 300 K under which conditions⁹ $\sigma_{\text{expt}}=3 \times 10^{-4} \Omega^{-1} \text{cm}^{-1}$, and

$$E_b \gtrsim \begin{cases} 0.38 \text{ eV} & \text{if } n < 1 \\ 0.6 \text{ eV} & \text{if } n = 1. \end{cases} \quad (66)$$

Finally, we note that these values are inconsistent with the observed room-temperature value of the thermopower or the log derivative of the conductivity, both of which yield apparent conductivity activation energies of 0.3 eV.

V. COMPARISON WITH EXPERIMENT

Comparison between theory and experiment is difficult in polyacetylene, both because of the theoretical uncertainties discussed in Sec. III and IV, and due to experimental uncertainties associated with the characterization of the samples. For instance, the extent to which putatively undoped samples are actually accidentally doped is uncertain.³³ (That they are always p type and compensatable argues for at least some trace-acceptor concentration.) The doping efficiency (the extent of charge transfer) of the various impurities that are used for doping is another important example of an experimental uncertainty. (That the same concentration of two different dopant species can produce different magnitudes of the conductivity argues that charge transfer can be less than one per impurity.) Thus, for the purposes of this discussion, we will divide the predictions of the theory into those qualitative predictions that depend only on the structure of the theory of hopping conduction, and the more quantitative predictions that depend on the details of the calculations.

The first class of predictions are listed in Table II. The model predicts that the temperature dependence of the conductivity (prediction 1) and thermopower (prediction 7) are roughly independent of dopant concentration. (The same is true of free-soliton conduction where S and the temperature dependence of σ are determined by the thermal population of free solitons, and hence by E_b alone.) Both predictions 1 and 7 seem to have been confirmed experimentally in lightly doped polyacetylene. For instance, in Br-doped polyacetylene¹¹ the conductivity can be increased by over 1.5 orders of magnitude by introducing 1 Br for every 170 C atoms ($y_{\text{Br}}=0.0059$) without making an observable change in the temperature depen-

dence of σ . The thermopower is found to be constant in magnitude (within experimental error) up to an I_3 concentration of a couple tenths of a percent.⁹

Prediction 2, the subactivated behavior of σ , distinguishes between hopping and free-soliton conduction. Although at low dopant concentrations the conductivity can only be measured over a rather limited range of temperatures, there seems to be general agreement^{9,11,14} that σ decreases more slowly than $e^{-E_b/k_B T}$. This nonactivated behavior is illustrated still more clearly by the experimentally observed⁹ approximate temperature independence of S (in agreement with prediction 6). The measured conductivity is a strongly increasing function of impurity concentration (prediction 3); it rises by almost 3 orders of magnitude as the AsF_5 concentration is raised from 0.3% to 0.6%. Without an extremely accurate determination of the accidental dopant concentration and a method for determining unambiguously the concentration of neutral solitons in doped samples, it is impossible to determine whether the conductivity obeys a $\ln \sigma \sim c_{\text{imp}}^{-1/3}$ law.

Non-Ohmic behavior of the conductivity (prediction 4) has been observed¹⁵ in 0.5% AsF_5 -doped samples at relatively low electric-field strengths. From the strength of the field \mathcal{E}_0 , at which non-Ohmic behavior sets in, it was found to be possible to deduce experimentally a characteristic hopping distance $R_{\text{char}} \sim 60 \text{ \AA}$ by using the relation in Eq. (44a). A theoretical estimate of R_{char} at $y=0.5\%$ can be obtained from Eq. (44b): $R_{\text{char}} \approx 35 \text{ \AA}$. If the charge transfer on doping is incomplete (see discussion below) a still higher value of R_{char} is obtained. We thus conclude that the theoretical value of \mathcal{E}_0 is in rough agreement with experiment. For field strengths greater than \mathcal{E}_0 , the electric-field-dependent conductivity is found to obey the approximate expression $\sigma \sim \sigma_0 \exp(\mathcal{E}/\mathcal{E}_0)$. Whether or not this observation is consistent with theory must be determined on the basis of further theoretical calculations.

Further experiments are necessary before even a qualitative comparison between theory and experiment can be made with any degree of confidence regarding predictions 5, 8, and 10. Nonetheless, such sketchy results as do exist seem to support the hopping picture.

Measurements¹⁶ of the ac conductivity from 10 to 10^7 Hz show no appreciable frequency dependence, but a factor of 500 enhancement of the conductivity has been observed¹² in undoped and light-

TABLE II. Predictions of the hopping-conduction picture with experiment in polyace-

| Predictions of the theory | Experiment |
|---|--|
| Conductivity: | |
| (1) Temperature dependence of σ is independent of dopant concentration at very low dopant concentrations | Confirmed for $y_{Br} \leq 0.6\%$ |
| (2) σ is more slowly varying with temperature than $\exp(-E_b/k_B T)$ [$\ln\sigma \sim (a+1)\ln T$] | Apparently confirmed |
| (3) σ is very rapidly increasing with impurity concentration ($\ln\sigma \sim c_{imp}^{-1/3}$) | Consistent with theory |
| (4) Non-Ohmic behavior at relatively low electric fields ($\mathcal{E} \geq k_B T/eR_{char}$) | Consistent with theory |
| (5) Strongly frequency dependent $\sigma(\omega)$ [$\sigma(\omega) - \sigma_{dc} \sim \omega(\ln\omega)^4$] | Not inconsistent |
| Thermopower: | |
| (6) S is very weakly temperature dependent ($S \sim e/k[\text{const} + \ln(k_B T/\hbar\omega_1)]$) | Consistent with theory |
| (7) S is only weakly impurity-concentration dependent ($S \sim e/k[\text{const} + \ln(y_n/y_{ch})]$) | Consistent with theory |
| Hall mobility: | |
| (8) Small but finite | No experiments |
| Spin-diffusion constant: | |
| (9) The dominant in-chain spin-diffusion mechanism is unrelated to, and more efficient than the conduction mechanism ($e^2 c_{imp} D \gg k_B T \sigma$) | Consistent with theory |
| (10) D_1 is related to σ by an Einstein relation ($e^2 c_{imp} D_1 = k_B T \sigma$) | Preliminary results are consistent with theory |

ly doped polyacetylene at a frequency of $\omega = 1.0 \times 10^{10}$ Hz. To see if this behavior is consistent with the dispersion predicted by Eq. (42) (prediction 5), we estimate the frequency ω_{ac} at which the conductivity is expected to begin to show a substantial frequency dependence. ω_{ac} is defined implicitly by the expression

$$[\sigma(\omega_{ac}) - \sigma_{dc}] / \sigma_{dc} = 1.$$

For $y = y_0 = 0.3\%$ and $\sigma_{ac} \sim 2 \times 10^{-6} \Omega^{-1} \text{cm}^{-1}$, we find that $\omega_{ac} \sim 10^8$ Hz. We therefore conclude that Eq. (42) is consistent with experiment, but further experiments in the frequency range 10^8 to 10^{10} Hz are necessary to verify the form of the frequency dependence in Eq. (42).

A spin-diffusion rate, both in-chain, $\nu \approx 6 \times 10^{13}$

Hz, and out of chain, $\nu_1 \leq 6 \times 10^7$ Hz, have been determined for undoped polyacetylene from measurements of the nuclear relaxation rate.¹³ It has been assumed that these rates are proportional to the spin-diffusion constant, and in particular that $D_1 = b^2 \nu_1$. We will adopt this relation for the purposes of discussion without attempting to justify it.

The extreme anisotropy of the spin-diffusion constant is evidence of a highly one-dimensional, mobile spin carrier, such as the neutral soliton. There is evidence³⁴ that the spin-diffusion constant is not related to the conductivity by an Einstein relation, and in particular, if an accidental impurity concentration of a few hundred ppm is assumed, $e^2 c_{imp} D_{||} \gg k_B T \sigma$ (consistent with prediction 9). This strongly suggests that charge transport and

in-chain spin transport occur via distinct mechanisms. On the other hand, prediction 10 implies that the magnitude of D_{\perp} can be deduced from the magnitude of σ . A typical⁹ room-temperature value for σ is $2 \times 10^{-5} \Omega^{-1} \text{cm}^{-1}$. If we assume that there is an accidental dopant concentration of about $y_{\text{ch}} = 4 \times 10^{-4}$ (see discussion below), we can obtain theoretical estimate of D_{\perp} from Eq. (45):

$$D_{\perp}/b^2 \approx 10^7 \text{ Hz},$$

which is in fair agreement with the measured value. Further measurements of D_{\perp} as a function of temperature and impurity concentration could provide a crucial test of the theory.

Quantitative comparison between the calculated and experimental thermopower in the hopping regime is relatively straightforward. Experimentally, the thermopower⁹ is found to be about $850 \mu\text{V}/\text{K}$ in undoped samples. The theoretically predicted value for $y_{\text{ch}} \sim y_n$, $S = 500 \mu\text{V}/\text{K}$, is in good agreement with experiment in light of the crude approximations that went into calculating $\bar{\epsilon}$.

The theoretical room-temperature hopping conductivity, as a function of impurity concentration y , is shown in Fig. 4. To obtain a value for the typical hopping distance [see Eq. (36)] as a function of y requires a knowledge of the mean volume V per CH_x . V , in turn, depends on the three-dimensional structure of the CH_x chains. If we assume the chains resemble close-packed cylinders, $V = ab^2$ (curve 1). An alternative estimate of V can be obtained empirically in two ways. If the sample is assumed to be a homogeneous medium, then from the measured⁹ density of polyacetylene ($0.4 \text{ g}/\text{cm}^3$), a value $V = 2.3ab^2$ is obtained (curve 2). However, it is known that polyacetylene has a fibrous structure, with the fibers filling about $\frac{1}{3}$ of the volume. If the mean density is corrected for the filling fraction, then the revised estimate $V = 0.77b^2a$ is obtained (curve 3). We will adopt the theoretical value for V (curve 1) for the purposes of this discussion, but Fig. 4 should serve as a warning concerning the ambiguity inherent in this assignment. Also shown in Fig. 4 are the measured conductivities for various concentrations of AsF_5 and Br. The measured conductivities are somewhat smaller than the theoretical values. This may be due to a variety of causes, such as the disordered topology of the actual polyacetylene or the electron-electron interactions discussed in the next section. However, the prime source of disagreement between theory and experiment is probably the incomplete charge transfer. We ex-

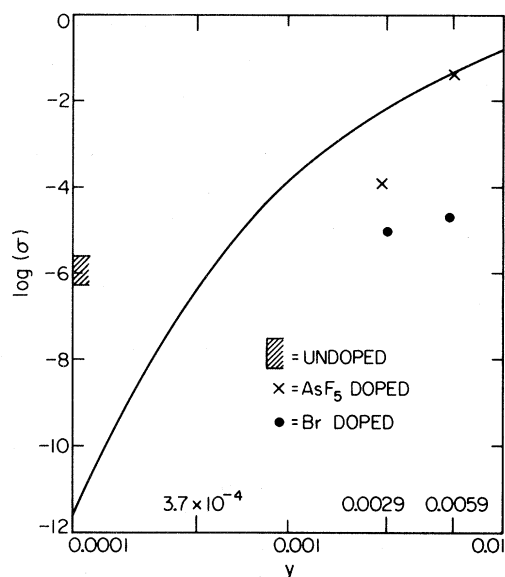


FIG. 4. Conductivity as a function of impurity concentration at 250 K. The solid curve is the theoretical conductivity for close-packed polyacetylene chains. The shaded region is the range of experimentally observed conductivities in undoped samples (from Refs. 9 and 11). The \times 's are experimental conductivities for AsF_5 -doped samples (from Ref. 9); the \bullet 's are for Br-doped samples (from Ref. 11).

pect, in general, less than one charge to be transferred per dopant atom. In Br-doped samples, for instance, some Br may be incorporated as Br_2 or Br_3 molecules, reducing substantially the doping efficiency. The lowest room-temperature conductivity reported in undoped trans CH_x is about $3 \times 10^{-6} \Omega^{-1} \text{cm}^{-1}$, corresponding to a putative "accidental" doping concentration of about $y = 4 \times 10^{-4}$. This is somewhat larger than the value estimated by other techniques,³³ $y \sim 10^{-4}$, but not disastrously so in view of the crudeness of both estimates.³⁵

Implicit in the calculation of the conductivity is the assumption that there exists a finite density of neutral solitons even in doped samples. This has apparently been confirmed experimentally since the neutral solitons give rise to a Curie-law susceptibility, and a roughly constant density of neutral solitons¹⁰ $y_n \sim 3 \times 10^{-4}$ at dopant concentrations up to tenths of a percent has been deduced from the magnitude of the susceptibility. At higher concentrations some of the electronic states become delocalized over many solitons and the number of neutral solitons is no longer simply related to the mag-

nitude of the susceptibility.⁸ We have thus made the assumption that the concentration of neutral solitons is independent of the dopant concentration at all relevant doping levels.¹⁷ Since σ depends only linearly on y_n , none of the results are terribly sensitive to this assumption.

Finally, in Fig. 5, the temperature dependence of the conductivity is compared to that measured in variously doped $(\text{CH})_x$ samples. The agreement is satisfactory. Note that none of the theoretical curves obtained in this section contain any adjustable parameters.

VI. MISSING FROM THE MODEL

The calculations reported in this paper are obviously greatly simplified. Effects of the detailed structure of the electron-phonon coupling function $g(E)$ can be included in a straightforward manner in a future calculation when the phonon wave functions become available. Although the results of such a calculation will undoubtedly lead to a rather more complicated temperature dependence of the conductivity than that in Eqs. (38) and (57), the qualitative aspects of the present calculations will probably survive that more detailed analysis.

Potentially more serious in terms of their possible qualitative effects are the electron-electron and soliton-soliton interactions that we have ignored. The repulsion between electrons in the same soliton bound state has little effect on the hopping process since the number of doubly occupied solitons is conserved in each hop. (The repulsion has been

taken into account implicitly, in that hops which convert two neutral solitons into a positively and a negatively charged soliton have been excluded.) The repulsion between electrons bound to different solitons leads to an effective charged-soliton—charged-soliton repulsion. In calculating the hopping rate between solitons, we treated all impurities as equivalent. However, there is a high probability that a given impurity has an oppositely charged soliton bound to it. Such an impurity appears less attractive to a charged soliton on another, neighboring chain. Thus, the electron-electron interaction leads to further (energy) disorder in the problem. A similar phenomenon occurs in lightly doped crystalline semiconductors. There, the electron-electron interaction can lead to a “Coulomb gap,” which results in a reduced conductivity. At low temperatures, it can lead to complicated, coherent multielectron hops.³⁶

Two solitons on the same chain interact strongly when their distortion fields overlap. A neutral soliton and a charged soliton attract each other, and form a bound, single-charged-soliton—antisoliton pair which resembles a polaron in conventional semiconductors. Within the SSH model the binding energy of the pair is about 0.3 eV.⁶ A charged and a neutral soliton on neighboring chains also attract each other, although more weakly. This attraction is due to the ability of an electron in a midgap state to delocalize over two solitons, similar to the bonding of a H_2^+ ion. Within the three-dimensional model discussed in Sec. III, the binding energy of this complex is t_1 . Since generally the charged soliton is bound to an impurity, the soliton-soliton interactions can be viewed as giving rise to an effective neutral soliton-impurity attraction. Thus, the assumption that leads to Eqs. (18) and (19), that the energy of the neutral soliton can be ignored, is called into question. In particular, the assumption that the neutral solitons are not bound to impurities breaks down at low temperatures. If $\Delta E^{(\text{eff})}$ is the effective binding energy of a neutral soliton to an impurity, then most of the neutral solitons will be “free” so long as

$$k_B T > \Delta E^{(\text{eff})} / |\ln y| .$$

For $\Delta E^{(\text{eff})} \approx t_1 \approx 0.1$ eV and $y \sim 0.1\%$, this restricts us to temperatures in excess of about 150 K. At lower temperatures, we expect an enhancement of the conductivity due to the increasing probability of finding a neutral soliton near an impurity.

Finally, there are significant sources of disorder in actual $(\text{CH})_x$ samples in addition to the solitons

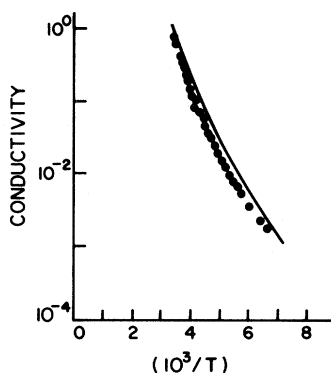


FIG. 5. Conductivity as a function of temperature (normalized at room temperature). The dots are the measured conductivity in an AsF_5 -doped ($y=0.0029$) sample (from Ref. 9), and the solid line is the theoretical temperature dependence.

and the charged impurities. For example, $(\text{CH})_x$ forms cords of about 200 Å in diameter which form a disordered, fibrous structure filling about $\frac{1}{3}$ of the volume of the sample. This additional large-scale disorder certainly leads to a decrease in the conductivity relative to that of "ideal," dense polyacetylene.

VII. COMPARISON WITH OTHER HOPPING MODELS

In this final section some of the most important qualitative differences between the present hopping model and other hopping models will be examined in an attempt to determine the extent to which the experimental results in $(\text{CH})_x$ can distinguish among the various models.

If we focus exclusively on the transport, there are several general features that any hopping model must have in order to be compatible with experiment. The strong dependence of the conductivity on doping concentration and the finding that the conductivity can be quenched by compensating with small amounts of NH_3 , imply that the hopping sites must be associated with the charged impurities. Moreover, the strong, nonactivated temperature dependence of σ implies that there must be a wide range of activation energies for hopping, either due to dynamical disorder, as in the present model or in small polaron hopping, or due to static disorder, as in variable-range hopping. Hence, we will consider these three models.

Perhaps the strongest support for the present model comes from the experimental results which implicate the neutral soliton in the transport mechanism. As mentioned before, the extremely anisotropic spin-diffusion constant is one such result. This anisotropy is probably too great to be due simply to the anisotropic mobility of a conventional free electron in $(\text{CH})_x$. Equally striking is the dependence of the conductivity on isomerization. When a sample of *cis*- $(\text{CH})_x$ is isomerized to *trans*- $(\text{CH})_x$, its conductivity rises by more than 6 orders of magnitude.³⁷ The concentration of charged impurities is clearly unaffected by isomerization. Moreover, by compensating the *trans* sample, conductivities approaching those in the *cis* can be regained. This remarkable behavior is easily understood in the present model. There are no mobile neutral solitons in the *cis* and no charged solitons in the compensated *trans*. Hence, in both these cases any conduction mechanism involving

solitons is "frozen out," and another, presumably less efficient mechanism, such as variable-range hopping in intrinsic midgap states, must account for the residual conductivity. Any hopping model that does not implicate neutral solitons is hard pressed to explain this behavior. It also may be possible in the future to test the $1/N$ dependence of the conductivity in Eq. (2). This dependence results from the involvement of the neutral soliton in the hopping and is probably unique to the present model.

To make a more detailed analysis, we next compare the predictions of the present model with those of a model of variable-range hopping with weak electron-phonon interactions (i.e., the polaron binding energy is small compared to the typical hopping energy.) The strongest evidence against variable-range hopping comes from measurements of the thermopower. For variable-range hopping in three dimensions, the thermopower is weakly temperature dependent³⁸:

$$S \sim (k/e)^{\frac{1}{2}} \sqrt{T/T_0} \frac{d \ln N(E)}{dE}, \quad (67)$$

where $T_0 \propto 1/c_{\text{imp}}$ and $N(E)$ is the density of states at the Fermi level. The weak temperature dependence of Eq. (67) is not clearly inconsistent with experiment, but the concentration dependence is. In particular, when the band of localized states is more than half-full, as it most certainly is in doped samples, $d \ln N(E)/dE$ is expected to be negative. Hence, Eq. (67) would predict a negative thermopower for *p*-type samples and an extremely small magnitude of the thermopower since $d \ln N(E)/dE \sim 0$ in the most lightly doped samples. Experimental results are in disagreement with both of these predictions but are in satisfactory agreement with the predictions of Eq. (35). Further evidence against variable-range hopping comes from the temperature dependence of the ac conductivity. The ac conductivity for variable-range hopping is given by a formula³⁸ of the same form as Eq. (42) with Γ_0 replaced by a roughly temperature-independent frequency ν_0 of the order of a phonon frequency and $(c_{\text{imp}})^2$ replaced by $[N(E)k_B T]^2$. Thus, the ac conductivity for variable-range hopping is weakly (linearly) dependent on T . The dynamical nature of the disorder in the present model (or in a model of small-polaron hopping) produces a much more strongly temperature dependent $\sigma(\omega)$, through the T dependence of Γ_0 . [Note that $\sigma(\omega)$ is still much more weakly T dependent than σ_{dc} .] Recent measure-

ments of Epstein *et al.*³⁷ reveal a strongly T -dependent ac conductivity in qualitative agreement with the present model.

The other model to be considered is small-polaron hopping in a narrow polaron band. Aside from the question of the origin of such a band, the most serious difficulty with this model is in explaining the sensitivity of the conductivity to isomerization. The behavior of the thermopower is also hard to account for in this model since in most simple models of small-polaron hopping the energy current is zero, and the same problems arise which were discussed above in the context of variable-range hopping. However, Emin²³ has shown that for certain models an energy-current contribution can arise from polaron hopping.

Finally, a further reason for preferring the present model should be mentioned. There is considerable evidence from other, nontransport experiments (summarized, for instance, in Ref. 39) which supports the soliton model. Thus, it is gratifying to obtain a successful explanation of the transport in terms of the same, simple model.

ACKNOWLEDGMENTS

It is a pleasure to acknowledge the help and guidance of Professor J. R. Schrieffer and a number of invaluable discussions with Professor A. J. Heeger and Dr. S. Etemad. This work was supported in part by National Science Foundation Grant No. DMR80-07432.

APPENDIX A: HOPPING CONDUCTION AND DIMENSIONALITY

Consider a d -dimensional disordered system in which an electron hops between impurity sites separated by a vector \vec{R} at a rate

$$\gamma = \gamma_0 e^{-2(R_{\parallel}^2/\xi_{\parallel}^2 + R_{\perp}^2/\xi_{\perp}^2)^{1/2}}, \quad (\text{A1})$$

where \vec{R} is the $(d-1)$ -dimensional component of \vec{R} perpendicular to the "easy" or parallel direction. It is convenient to express the hopping statistics in terms of the function $N_d(\gamma)$, which is the mean number of sites to which the hopping rate from a given site (the origin) is greater than γ :

$$N_d(\gamma) = A_d C_d \left[\frac{\xi_{\parallel}}{2} \right] \left[\frac{\xi_{\perp}}{2} \right]^{d-1} [\ln(\gamma_0/\gamma)]^d, \quad (\text{A2})$$

where $A_d R^d$ is the volume of a d -dimensional

sphere of radius R and C_d is the concentration of impurities.

The important statistical properties of the hopping can be derived from $N_d(\gamma)$. For instance, the conductivity is predominantly determined by the hopping rate γ_c which defines the percolation network. Specifically, γ_c is the largest rate such that if all rates less than γ_c were arbitrarily set equal to zero, it would still be possible for an electron to hop across an infinite system. γ_c is determined by the equation

$$P_d = N_d(\gamma_c), \quad (\text{A3})$$

where P_d is the d -dimensional percolation fraction, which is roughly 2.71 in three dimensions.²⁰ Thus,

$$\gamma_c = \gamma_0 e^{-2BR_0/\xi}, \quad (\text{A4})$$

where $B = (P_d)^{1/d}$, R_0 is the typical separation between sites,

$$R_0 = (A_d C_d)^{1/d}, \quad (\text{A5})$$

and ξ is the dimensionally averaged decay length

$$\xi = (\xi_{\parallel} \xi_{\perp}^{d-1})^{1/d}. \quad (\text{A6})$$

Equation (B4) contains the most rapid dependence of the conductivity on concentration. To derive the proper prefactors in Eqs. (2) and (38), the approximation scheme of Butcher *et al.*²⁰ must be used. The result in Eq. (38) follows in a straightforward manner from that analysis.

In polyacetylene, there is intrinsic graininess to the problem in that the polyacetylene chain has a finite radius. The conductivity in Eq. (38) was derived ignoring this graininess. Given a three-dimensional concentration of sites C_3 , the graininess can only be ignored if most hops are between different chains, not on the same chain. To examine this question, we compare the distribution of three-dimensional (3D), or interchain hop rates, with the distribution of intrachain, or one-dimensional hop rates. The one-dimensional (1D) concentration of sites on a single chain is related to C_3 by the expression

$$C_1 = C_3 \Omega, \quad (\text{A7})$$

where Ω is the cross-sectional area per polyacetylene chain. If we assume that the chains are close-packed,

$$\Omega = b^2, \quad (\text{A8})$$

where b is the interchain separation. From the analytic form of Eq. (B2), it is clear that for γ

large, that is γ near γ_0 , $N_1(\gamma) > N_3(\gamma)$, while for small γ , $N_3(\gamma) > N_1(\gamma)$. Thus, the crossover from 1D to 3D behavior can be defined in terms of the hopping rate $\bar{\gamma}$,

$$\ln(\gamma_0/\bar{\gamma}) = \left[\frac{3}{\pi} \right]^{1/2} \left[\frac{b}{\xi_{\perp}} \right], \quad (\text{A9})$$

which is chosen such that

$$N_3(\bar{\gamma}) = N_1(\bar{\gamma}) = C_3 b^3 \frac{\xi_{\parallel}}{2\xi_{\perp}} \left[\frac{3}{\pi} \right]^{1/2}. \quad (\text{A10})$$

At low concentration, that is for $N(\bar{\gamma}) \ll 1$, most sites have an off-chain neighbor to which an electron can hop more readily than to the nearest on-chain neighbor. In fact, $N(\bar{\gamma})$ is approximately the fraction of sites from which an electron is more likely to make an intrachain hop than an interchain hop. Effects of the graininess become important when $\bar{\gamma} \gtrsim \gamma_c$ or in other words when $N_3(\bar{\gamma}) \gtrsim P_3$. However, for the systems considered in this paper, $N_3(\bar{\gamma}) \ll 1$, so the graininess is relatively unimportant.

APPENDIX B: THE OUT-OF-CHAIN DECAY OF THE SOLITON BOUND STATE

In this appendix we consider the properties of a localized midgap state in the three-dimensional model of crystalline polyacetylene of Sec. III. For perfect dimerization, the system is described by the Hamiltonian:

$$H = \sum_l \sum_{ns} \left[(t_0 + \frac{1}{2} \Delta_0) (c_{l,2n,s}^{\dagger} c_{l,2n+1,s} + \text{H.c.}) + (t_0 - \frac{1}{2} \Delta_0) (c_{l,2n,s}^{\dagger} c_{l,2n-1,s} + \text{H.c.}) \right] + \sum_{ns} \sum_{\langle ll' \rangle} [\tilde{t}_{\perp} (l-l') (c_{l,n,s}^{\dagger} c_{l',n,s} + \text{H.c.})]. \quad (\text{B1})$$

Here the sites are identified according to the convention used in Sec. III and the final sum in Eq. (C1) is over nearest-neighbor chains. The eigenstates of this system are block waves with energies

$$E_{\pm}(k_{\parallel}, \vec{k}_{\perp}) = \pm \epsilon(k_{\parallel}) + t_{\perp}(\vec{k}_{\perp}), \quad (\text{B2})$$

where

$$\epsilon(k_{\parallel}) = [(2t_0)^2 \cos^2(k_{\parallel}a) + \Delta_0^2 \sin^2(k_{\parallel}a)]^{1/2}, \quad (\text{B3})$$

and

$$t_{\perp}(\vec{k}_{\perp}) = \sum_{\vec{l}} \tilde{t}_{\perp}(\vec{l}) e^{i \vec{k}_{\perp} \cdot \vec{l}}, \quad (\text{B4})$$

and \vec{l} is the displacement vector between nearest-neighbor chains. For analytic convenience, we will consider a two-dimensional crystal so that the small dependence of E on the direction of \vec{k}_{\perp} can be ignored. Thus,

$$t_{\perp}(\vec{k}) \approx 2t_{\perp} \cos(k_{\perp}b), \quad (\text{B4}')$$

where k_{\perp} varies between $\pi/b < k_{\perp} < \pi/b$.

So long as $\Delta_0 > 2t_{\perp}$, there exists a band gap about zero energy. The asymptotic decay of a localized state in the band gap is determined by the decay of the one-particle Green's function $G(E; \vec{R})$ at $E=0$ (see Ref. 25). By combining Eqs. (B2) to (B4) we obtain an expression for G :

$$G(E; R_{\parallel}, R_{\perp}) = \int_{-\pi/2a}^{\pi/2a} \frac{dk_{\parallel}}{2\pi} e^{ik_{\parallel}R_{\parallel}} \int_{-\pi/b}^{\pi/b} \frac{dk_{\perp} e^{ik_{\perp}R_{\perp}}}{\pi} \left[\frac{1}{E - \epsilon(k_{\parallel}) - t_{\perp}(k_{\perp})} + \frac{1}{E + \epsilon(k_{\parallel}) - t_{\perp}(k_{\perp})} \right]. \quad (\text{B5})$$

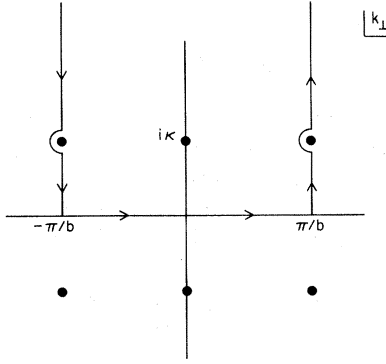
The k_{\perp} integral can be performed by integrating around the contour shown in Fig. 6. At $E=0$,

$$\int_{-\pi/b}^{\pi/b} \frac{dk_{\perp} e^{ik_{\perp}R_{\perp}}}{\pi} e^{ik_{\perp}R_{\perp}} = \frac{-e^{-\kappa R_{\perp}}}{2t_{\perp} \sinh(\kappa b)},$$

where

$$\kappa b = \cosh^{-1}[\epsilon(k_{\parallel})/2t_{\perp}].$$

For $R_{\parallel}=0$ and R_{\perp} large, the leading term in G

FIG. 6. Contour of integration in the k_{\perp} plane

can be obtained by expanding the integrand about $k_{\parallel} = \pm\pi/2$:

$$G(0;0,R) = \left(\right) \frac{e^{-\kappa_0 R_{\perp}}}{(\kappa_0 R_{\perp})^{1/2}} \left[1 + O \left[\frac{1}{(\kappa_0 R)} \right] \right],$$

where $()$ is an R_{\perp} -independent constant and

$$b\kappa_0 = \cosh h^{-1}(\Delta_0/2t),$$

or, for $\Delta_0 \gg t_{\perp}$,

$$\xi_{\perp} \approx b/\ln(\Delta_0/t_{\perp}).$$

If, instead, we set $R_{\perp} = 0$ and consider R_{\parallel} large, then

$$G(0;R_{\parallel},0) = \int_{-\pi/2a}^{\pi/2a} \frac{dk_{\parallel} e^{ik_{\parallel} R_{\parallel}}}{\pi[\epsilon^2(k_{\parallel})/2t)^2 - 1]^{1/2}}.$$

The principle contribution to the integral comes from the vicinity of the singularity in the integrand at $\epsilon(ik_{\parallel}) = 2t_{\perp}$, so $G(0;R_{\parallel},0) \sim e^{-\kappa_{\parallel} R_{\parallel}}$ where for $\Delta_0 \gg 2t_{\perp}$,

$$\kappa_{\parallel}^{-1} = \xi_{\parallel} = a \left[\frac{2t_0}{\Delta_0} \right] \left[1 + O \left[\left[\frac{2t_{\perp}}{\Delta_0} \right] \right]^2 \right].$$

Thus, we recover the one-dimensional result quoted in Sec. III.

APPENDIX C: MULTIPHONON TRANSITION RATES

In this appendix we sketch the formal calculation of the phonon-assisted transition rate between two solitons, that is, we *drop* the assumption made in Sec. II that $\Lambda_{\alpha}^{(i)} = 0$. The remarkable result is that so long as $\bar{p}_2(\epsilon_2)$ in Eq. (11) is a slowly varying function of ϵ_2 on the scale of the polaron bind-

ing energy, multiphonon processes do not have a large affect on the total transition rate, ν .

To do the calculation it is convenient to transform to polaronic coordinates (see, e.g., Ref. 19):

$$\begin{aligned} B_{\alpha} &= e^s b_{\alpha} e^{-s}, \\ A_i &= e^s a_i e^{-s}, \end{aligned} \quad (C1)$$

where

$$S = \sum_{\alpha} \sum_{i=1}^2 \Lambda_{\alpha}^{(i)} a_i^{\dagger} a_i (b_{\alpha}^{\dagger} - b_{\alpha}).$$

In terms of the transformed variables, the reduced Hamiltonian in Eq. (7) becomes

$$\begin{aligned} H^{(\text{red})} &= \sum_{i=1}^2 E_i A_i^{\dagger} A_i + \sum_{\alpha} \hbar\omega_{\alpha} (B_{\alpha}^{\dagger} B_{\alpha} + \frac{1}{2}) \\ &+ \sum_{i=1}^2 [V(x_i) A_i^{\dagger} A_i + T(x_i)] \\ &+ \sum_{\alpha} \hbar\omega_{\alpha} \lambda_{\alpha} (B_{\alpha}^{\dagger} - B_{\alpha}) (e^{\theta} A_1^{\dagger} A_2 + \text{H.c.}), \end{aligned} \quad (C2)$$

where $E_i = \mathcal{E}_i^{(0)} - E_p^{(i)}$, $E_p^{(i)}$ is the polaron binding energy

$$E_p^i = \sum_{\alpha} \hbar\omega_{\alpha} (\Lambda_{\alpha}^{(i)})^2, \quad (C3)$$

and

$$\theta = \sum_{\alpha} (\Lambda_{\alpha}^2 - \Lambda_{\alpha}^{(1)}) (B_{\alpha}^{\dagger} - B_{\alpha}).$$

Then, from Fermi's golden rule we obtain Eq. (11), where

$$\begin{aligned} \nu_{12} &= \frac{2\pi}{\hbar} \sum_{AB} \frac{e^{-E_A/k_B T}}{Z_{\text{ph}}} |\langle A | F | B \rangle|^2 \\ &\times \delta(\epsilon_2 - \epsilon_1 + E_B - E_A), \end{aligned} \quad (C4)$$

$$F = \sum_{\alpha} \hbar\omega_{\alpha} \lambda_{\alpha} (B_{\alpha}^{\dagger} - B_{\alpha}) e^{-\theta}, \quad (C5)$$

where $\{|A\rangle\}$ and $\{|B\rangle\}$ are a complete set of phonon states and $Z_{\text{ph}} = \sum_A e^{-E_A/k_B T}$ is the phonon partition function. We must distinguish between two types of phonons in the expression for θ : (1) localized phonons (the shape mode) of which there is one per soliton with energy¹ $\hbar\omega_1 \sim 0.09$ eV, and (2) delocalized modes for which $\Lambda_{\alpha} \sim 1/\sqrt{\Omega}$ where Ω is the volume of the system.

Because $\hbar\omega_1$ is so large, processes involving the absorption and emission of these phonons are largely frozen out at all reasonable temperatures. Thus, ignoring terms that are smaller by a factor of $1/\sqrt{\Omega}$, the sum in Eq. (C4) can be factored to yield

$$\begin{aligned} \nu_{12}(\epsilon_1 - \epsilon_2) = & \frac{2\pi}{\hbar} \sum_{\alpha} (\hbar\omega_{\alpha})^2 (\lambda_{\alpha})^2 \\ & \times \sum_{AB} \frac{e^{-E_A/k_B T}}{Z_{\text{ph}}} \\ & \times |\langle A | (B_{\alpha}^{\dagger} - B_{\alpha}) e^{-\theta} | B \rangle|^2 \\ & \times \delta(\epsilon_1 - \epsilon_2 + E_B - E_A), \quad (\text{C6}) \end{aligned}$$

$$\begin{aligned} \nu = & \frac{2\pi}{\hbar} \sum_{\alpha} \int d\epsilon_1 p_1(\epsilon_1) (\hbar\omega_{\alpha})^2 (\lambda_{\alpha})^2 \{ [1 + n(\hbar\omega_{\alpha})] [\bar{p}_2(\epsilon_1 - \hbar\omega_{\alpha}) - \overline{\Delta E} \bar{p}'_2(\epsilon_1 - \hbar\omega_{\alpha}) + \dots] \\ & + n(\hbar\omega_{\alpha}) [\bar{p}_2(\epsilon_1 + \omega_{\alpha}) - \overline{\Delta E} \bar{p}'_2(\epsilon_1 + \hbar\omega_{\alpha}) + \dots] \}, \quad (\text{C7}) \end{aligned}$$

where

$$\bar{p}_2^1(\epsilon) = d/d\epsilon \bar{p}_2(\epsilon),$$

and

$$\overline{\Delta E} = \sum_{AB} \frac{e^{-E_A/k_B T}}{Z_{\text{ph}}} |\langle A | e^{\theta} | B \rangle|^2 (E_B - E_Z). \quad (\text{8})$$

$\overline{\Delta E}$ is roughly the same size as E_p , and since E_b determines the scale of variation of \bar{p}_2 ,

$$\bar{p}'_2(\epsilon_2) \sim (1/E_b) \bar{p}_2(\epsilon_2).$$

where

$$|E_B - E_A| = \hbar\omega_{\alpha} + \Delta E_{AB}$$

and ΔE_{AB} is typically less than of order of the polaron binding energy. The expression in Eq. (C6) must be substituted into Eq. (11). If we make the assumption that $\bar{p}_2(\epsilon_2)$ does not vary much over a range of energies of order the polaron binding energy, then the sum over the intermediate phonon states can be carried out explicitly, and the factors of e^{θ} combine to give unity. To demonstrate the nature of the multiphonon corrections to the transition rate, we will keep the zeroth- and first-order terms in the Taylor expansion of $\bar{p}_2(\epsilon_2)$:

Thus, the change in ν due to the presence of multiphonon processes is expected to be of order $E_p/E_b \sim 0.1$ and hence small. Of course, any sharp features in the integrand of Eq. (11) which might otherwise lead to an activated temperature dependence of ν , will tend to be smoothed away by the presence of multiphonon processes.

Finally, we remark that the situation here is quite different from the more usual case of phonon assisted hopping between impurity sites, where $\bar{p}_2(\epsilon_2)$ is a δ function. In that case, as is well known, the multiphonon processes lead to an exponential suppression of the hopping rate at low temperature.

¹W. P. Su, J. R. Schrieffer, and A. J. Heeger, *Phys. Rev. Lett.* **42**, 1698 (1979); and *Phys. Rev. B* **22**, 2099 (1980).

²H. Takayama, Y. R. Lin-Liu, and K. Maki, *Phys. Rev. B* **22**, 2388 (1980).

³M. J. Rice, *Phys. Lett.* **71A**, 152 (1979).

⁴W. P. Su, *Solid State Commun.* **35**, 899 (1980).

⁵E. J. Mele and M. J. Rice (unpublished).

⁶W. P. Su and J. R. Schrieffer, *Proc. Nat. Acad. Sci. U. S. A.* **77**, 5626 (1980).

⁷S. Kivelson, *Phys. Rev. Lett.* **46**, 1344 (1981); W. P. Su, S. Kivelson, and J. R. Schrieffer, in *Physics in One Dimension, Springer Series in Solid-State Sciences*, edited by J. Bernasconi and T. Schneider (Springer, Berlin, 1980); S. Kivelson, *Mol. Cryst. Liq. Cryst.* **77**, 65 (1981).

⁸S. Kivelson (unpublished).

⁹Y. W. Park, A. J. Heeger, M. A. Druy, and A. G. MacDiarmid, *J. Chem. Phys.* **73**, 946 (1980); Y. W. Park, A. Denenstein, C. K. Chiang, A. J. Heeger, and A. G. MacDiarmid, *J. Chem. Phys.* **73**, 946 (1980).

¹⁰B. R. Wienberger, S. Kaufer, A. J. Heeger, A. Pron, and A. G. MacDiarmid, *Phys. Rev. B* **20**, 223 (1979); also S. Ikehata, J. Kaufer, T. Woerner, A. Pron, M. A. Druy, A. Sivak, A. J. Heeger, and A. G. MacDiarmid, *Phys. Rev. Lett.* **45**, 1123 (1980).

¹¹C. K. Chiang, Y. W. Park, A. J. Heeger, H. Shirakawa, E. J. Louis, and A. G. MacDiarmid, *J. Chem. Phys.* **69**, 5098 (1978).

¹²G. Milhaly, G. Vancso, S. Pekker, and A. Janossy, *J. Syn. Metals* **1**, 357 (1980).

¹³M. Nechtschein, F. Devreaux, R. L. Greene, T. C.

- Clarke, and G. B. Street, *Phys. Rev. Lett.* **44**, 356 (1980); F. Devreux, K. Holczer, M. Nechtschein, T. C. Clarke, and R. L. Greene, in *Physics in One Dimension*, Springer Series in Solid-State Sciences, edited by J. Bernasconi and T. Schneider (Springer, Berlin, 1980).
- ¹⁴Y. Tomkiewicz, T. D. Schultz, H. B. Bron, T. C. Clarke, and G. B. Street, *Phys. Rev. Lett.* **43**, 1532 (1979).
- ¹⁵K. Mortensen, M. L. W. Thewalt, Y. Tomkiewicz, T. C. Clarke, and G. B. Street, *Phys. Rev. Lett.* **45**, 490 (1980).
- ¹⁶P. M. Grant and M. Krounbi, *Solid State Commun.* **36**, 291 (1980).
- ¹⁷Su (Ref. 4) has shown that the ground state of a neutral $(\text{CH})_x$ chain contains a soliton if the chain has an odd number of carbons. Hence, we expect to find about one neutral soliton for every two chains in undoped polyacetylene. Similar considerations lead to the conclusion that in lightly doped samples, there will be a neutral soliton in the ground state of any chain in which the sum of the number of carbons and the number of charged solitons is odd. This may explain the seeming insensitivity of the number of Curie-law spins to the dopant concentration in lightly doped samples (see Ref. 8).
- ¹⁸SSH finds that it is energetically favorable to create a charged soliton rather than to introduce a free electron into the conduction band.
- ¹⁹R. Silbey, *Ann. Rev. Phys. Chem.* **27**, 203 (1976); A. Miller and S. Abrahams, *Phys. Rev.* **120**, 745 (1960).
- ²⁰E. Tomboulis, *Phys. Rev. D* **12**, 1678 (1975); see also T. Holstein, *Mol. Cryst. Liq. Cryst.* **77**, 235 (1981).
- ²¹The derivation of the electronic hopping rate between solitons ignores the interaction energy between a neutral soliton and a charged impurity. Although there is no electrostatic interaction, there is an indirect interaction via polarization of the electron cloud by the impurity. This interaction is probably very small and unimportant at all relevant temperatures. A more serious consideration is the indirect interaction of a neutral soliton with a charged impurity via its interaction with a charged soliton which is already bound to the impurity (on another neighboring chain) (see discussion in Sec. VI).
- ²²V. Ambegaokar, B. I. Halperin, and J. S. Langer, *Phys. Rev. B* **4**, 2612 (1971).
- ²³D. Emin, *Phys. Rev. Lett.* **35**, 882 (1975).
- ²⁴M. Pollack, *J. Non-Cryst. Solids* **11**, 1 (1972).
- ²⁵P. M. Butcher, K. J. Hauden, and J. A. McInnes, *Philos. Mag.* **36**, 19 (1977).
- ²⁶P. N. Butcher, J. D. Clark, A. Kumar, and J. A. McInnes, in *Amorphous and Liquid Semiconductors*, edited by W. Paul and M. Kastner (North-Holland, Amsterdam, 1980), p. 89.
- ²⁷L. Friedman and M. Pollak, *Philos. Mag. B* **38**, 173 (1978).
- ²⁸E. J. Mele, private communication.
- ²⁹The relativistic correction to the kinetic energy for a ϕ^4 soliton has been studied by J. A. Krumhansl and J. R. Schrieffer, *Phys. Rev. B* **11**, 3535 (1975). Reported there, the relativistic increase in mass is due to a contraction of the soliton, with $m = m_0[l(v)/l(0)]^2$, where $l(v)$ is the soliton width as a function of its velocity v . In a discrete model, $l(v)$ cannot be less than the lattice constant, a . Hence, the maximum relativistic correction is $(\xi_0/a)^2$.
- ³⁰It is normally assumed that $n_s = 1$. Only if the electron-electron interactions are large enough to exclude the possibility of two or more solitons (on different chains) being bound to the same impurity, is $n_c = 1$ and $n = 1$.
- ³¹ D_{ch} may depend on y , but it would be expected to be a decreasing function of y since the impurities will scatter free solitons.
- ³²Y. Wada and J. R. Schrieffer, *Phys. Rev. B* **18**, 3897 (1978).
- ³³M. Ozaki, D. Peebles, B. R. Weinberger, A. J. Heeger, and A. J. MacDiarmid, *J. Appl. Phys.* **51**, 4252 (1980).
- ³⁴G. Grunner, private communication.
- ³⁵A. J. Heeger, private communication.
- ³⁶See, for example, M. Pollak and M. L. Knotek, *J. of Non-Cryst. Solids* **32**, 141 (1979); and M. Pollak (unpublished).
- ³⁷A. J. Epstein, H. Rommelman, M. Abkowitz, and H. W. Gibson, *Mol. Cryst. Liq. Cryst.* **77**, 81 (1981).
- ³⁸N. F. Mott and E. A. Davis, *Electronic Processes in Non-Crystalline Materials* (Clarendon, Oxford, 1979).
- ³⁹A. J. Heeger and A. G. MacDiarmid, in *Springer Series in Solid-State Sciences*, edited by J. Bernasconi and T. Schneider (Springer, Berlin, 1980).